

MOLECULAR MECHANISM OF PHOTOSIGNALING BY ARCHAEAL SENSORY RHODOPSINS

Wouter D. Hoff, Kwang-Hwan Jung, and John L. Spudich

Department of Microbiology and Molecular Genetics, University of Texas Medical School, Houston, Texas 77030-1501

KEY WORDS: receptors, membrane protein interactions, signal transduction, phototaxis, chemotaxis, visual pigments

ABSTRACT

Two sensory rhodopsins (SRI and SRII) mediate color-sensitive phototaxis responses in halobacteria. These seven-helix receptor proteins, structurally and functionally similar to animal visual pigments, couple retinal photoisomerization to receptor activation and are complexed with membrane-embedded transducer proteins (HtrI and HtrII) that modulate a cytoplasmic phosphorylation cascade controlling the flagellar motor. The Htr proteins resemble the chemotaxis transducers from *Escherichia coli*. The SR-Htr signaling complexes allow studies of the biophysical chemistry of signal generation and relay, from the photobiophysics of initial excitation of the receptors to the final output at the level of the flagellar motor switch, revealing fundamental principles of sensory transduction and more broadly the nature of dynamic interactions between membrane proteins. We review here recent advances that have led to new insights into the molecular mechanism of signaling by these membrane complexes.

CONTENTS

OVERVIEW	224
PHOTOPHYSIOLOGY OF HALOBACTERIA	225
STRUCTURE AND FUNCTION OF SR-HTR COMPLEXES	227
<i>Structure of Sensory Rhodopsins</i>	228
<i>Color Regulation</i>	231
<i>Photochemical Reaction Cycle Intermediates</i>	233
<i>Identification of Receptor Signaling States</i>	234
<i>Structure of Sensory Rhodopsin Transducers</i>	235
SRI: STAGES IN SIGNALING	239
<i>From Photon Absorption to Signaling State</i>	239
<i>Stimulus Relay from the Signaling State to HtrI</i>	241
	223

<i>Transducer Activation and Adaptation: Two Signals</i>	244
<i>From Signaling Complex to the Flagellar Motor</i>	247
SRII: RECENT PROGRESS	247
INVERTED SIGNALING	248
PERSPECTIVES	250

OVERVIEW

Halobacteria, members of the domain Archaea, exhibit phototaxis responses to changes in light intensity and color by altering their swimming behavior. Sensory rhodopsins function as the photoreceptors modulating the reversal frequency of the cell's flagellar motors. These receptors, sensory rhodopsins I and II (SRI and SRII), convert light signals into biochemical information via associated transducer proteins (HtrI and HtrII), which in turn modulate a phosphotransfer pathway leading to the flagellar motor. This review covers the advances made since 1988 (141) in our understanding of photosensory transduction in this system¹.

Based on results summarized here, the SR and Htr proteins form complexes that function as molecular machines carrying out the following processes when exposed to a change in light intensity: The complex captures photons of a specific wavelength and stores the energy of the photons in a physico-chemical form in the photoactive site consisting of retinal and interacting protein residues. It uses the energy to populate states, called *signaling states*, which are structurally altered in regions of the receptor protein interacting with its bound Htr. The change in interaction is propagated to two distinct sites on the Htr protein, first to a region called the signaling domain, causing alteration of autophosphorylation activity of a bound histidine kinase (CheA),² and second to methylation regions, altering their susceptibility to methylation. Subsequently, a new level of methylation, established through the action of methyltransferase and methyl-esterase enzymes, apparently resets the activity of CheA to the prestimulus value in the continued presence of the signaling states. Therefore, the integrated output of the signaling complex is a transient change in kinase activity, resulting in a transient change in the phosphorylation level of a cytoplasmic regulator protein (CheY),² which in turn causes a transient alteration of the switching probability of the flagellar motor assembly. The commonly measured output is the transient change in swimming reversal frequency in a population of cells.

¹We attempt to refer to all published contributions to archaeal sensory rhodopsins that have appeared since the 1988 review (141). The authors of that review made a similar attempt to reference all contributions since the first report of a sensory rhodopsin in 1982. Here we do not refer to the literature before 1988, except where we consider it necessary to reference a specific result.

²The CheA and CheY proteins are named on the basis of their sequence homology to the *Escherichia coli* chemotaxis proteins (113) and putative function in mediating both chemotaxis and phototaxis signals in *Halobacterium salinarum*.

PHOTOPHYSIOLOGY OF HALOBACTERIA

Halobacteria inhabit the Dead Sea, solar evaporation ponds, and other regions of near to fully saturated brine (67). Solar radiation is intense in these habitats and the most studied species, *Halobacterium salinarum*, takes advantage of the two major roles played by light in the biosphere: as energy provider and as information carrier. *H. salinarum* membranes contain a family of four photoactive proteins, called archaeal rhodopsins (Figure 1), that are similar to our visual pigments in their structure and photochemistry: bacteriorhodopsin (BR; 98) and halorhodopsin (HR; 85, 124) harvest solar energy by electrogenic light-driven transport of protons and chloride, respectively, across the cytoplasmic membrane. SRI (16, 140) and SRII (152, 158) are phototaxis receptors that use the energy of absorbed photons to send signals to the flagellar motor

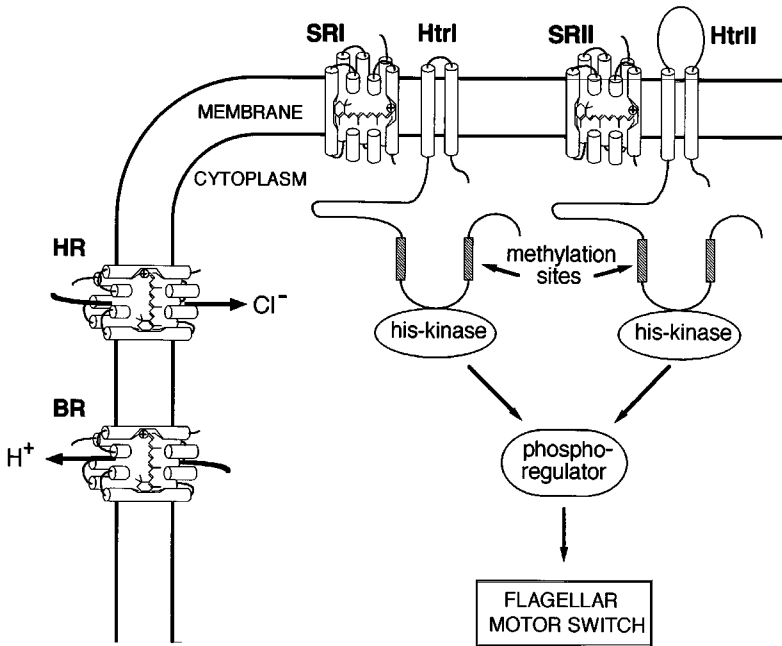


Figure 1 The four archaeal rhodopsins in *H. salinarum*. The transport rhodopsins BR (a proton pump) and HR (a chloride pump) are shown in addition to the sensory rhodopsins SRI and SRII with components in their signal transduction chains. Each rhodopsin consists of seven transmembrane α -helices enclosing a retinal chromophore linked through a protonated Schiff base to a lysine residue in the 7th helix. The sensory rhodopsins are complexed to their corresponding transducer proteins HtrI and HtrII, which have conserved methylation and histidine kinase-binding domains that modulate kinase activity, which in turn controls flagellar motor switching through a cytoplasmic phosphoregulator.

via HtrI (172) and HtrII (126, 174), respectively (HtrI/II stand for halobacterial transducers for sensory rhodopsin I and II).

The four archaeal rhodopsins and the three functions, proton transport, chloride transport, and phototaxis signaling, appear to account for retinal pigmentation and retinal-dependent functions in *H. salinarum*. Over 30 archaeal rhodopsins have been described and they all correspond in absorption spectrum and function to BR, HR, SRI, or SRII (92, 103, 104, 132). Several reviews are available on BR (26, 60, 66, 83, 112) and HR (65, 96). A comprehensive review of the earlier literature on halobacterial sensory rhodopsins can be found in a previous volume of this series (141), and a review covering both prokaryotic and eukaryotic microbial sensory rhodopsins has appeared recently (143). The functions of proton pumping, chloride pumping, and sensory signaling are distinctly different; nevertheless recent work reveals that modifications of the same versatile phototransduction machinery are responsible for these diverse consequences of photon absorption. Two recent minireviews focus on the comparison of transport and signaling (138, 142) and reviews on aspects of halobacterial phototaxis have appeared (97, 107, 137, 139).

Detailed analysis of the cells' movements in their natural habitat are not available, but from their physiology (46, 102, 120, 141, 153, 157, 159, 160) a plausible scenario can be constructed. *H. salinarum* grows at its maximum rate chemoheterotrophically in aerobic conditions (67). When oxygen and respiratory substrates are plentiful, *H. salinarum* cells would be expected to avoid sunlight and potential photooxidative damage. To accomplish this, they synthesize the repellent receptor SRII (also known as phoborhodopsin) as their only rhodopsin. SRII absorbs blue-green light in the energy peak of the solar spectrum at the Earth's surface. Hence, its wavelength sensitivity is tuned strategically to be maximally effective for seeking the dark.

A drop in oxygen tension suppresses SRII production and induces synthesis of BR and HR, enabling orange light absorbed by these pumps to be used as an energy source. Like the respiratory chain, BR pumps protons out of the cell, directly contributing to the inwardly directed proton motive force needed for ATP synthesis, active transport, and motility. HR is an inwardly directed pump, transporting chloride into the cell. Like cation ejection, anion uptake hyperpolarizes the membrane positive-outside. Therefore, the electrogenic inward transport of chloride contributes to the membrane potential component of proton motive force without loss of cytoplasmic protons. This transport helps maintain pH homeostasis by avoiding cytoplasmic alkalization.

Along with BR and HR, production of SRI is induced. SRI mediates attractant responses to orange light, facilitating migration into illuminated regions where the ion pumps will be maximally activated. SRI is endowed with a second signaling activity to ensure it will not perilously guide the cells into higher

energy light. A long-lived photointermediate of SRI, a species called S_{373} ,³ absorbs near-UV photons and mediates a strong repellent response. The color-sensitive signals from SRI, therefore, attract the cells into a region containing orange light only if this region is relatively free of near-UV photons. When back in a rich aerobic environment, the *H. salinarum* cells switch off BR, HR, and SRI synthesis and switch on SRII production.

Although the sensory rhodopsins are responsible for phototaxis under most conditions, some earlier work, especially action spectroscopy, suggested that BR could mediate attractant responses. Independent studies have confirmed attractant responses to orange light due to light-driven proton pumping by BR (11, 12, 162). The BR-mediated responses occur at high light intensities and are most evident in partially de-energized cells. Aerotaxis, which occurs in *H. salinarum* (145), has been attributed to proton motive force ($\Delta\mu_{\text{H}^+}^{\ddagger}$) or membrane potential ($\Delta\Psi$) changes (13, 69), and hence BR may also contribute via these parameters. A special cellular device measuring proton motive force, called a *protometer*, was proposed as the sensor (11). Alternatively, the BR-mediated responses may result from secondary consequences of electrogenic proton pumping (e.g. $\Delta\Psi$ changes) on metabolic or signal transduction pathways (37a, 162). The difference between these interpretations may be only semantic, if one accepts as a protometer a component(s) with a different primary function(s) in the cell.

Many other microorganisms also display protective photosensory responses (repellent phototaxis or induction of screening pigments) to blue light, although the receptors involved (called cryptochromes) are largely unknown (129). Recently, the *p*-coumaric acid-based (50) pigment photoactive yellow protein has been suggested to mediate repellent phototaxis in the phototrophic eubacterium *Ectothiorhodospira halophila* (133). In *Chlamydomonas reinhardtii* a retinal-binding receptor is responsible for both negative and positive phototaxis (32, 143). A gene was cloned recently that was proposed to encode the retinylidene receptor (Chlamyrodopsin) apoprotein (24). In addition, a gene homologous to a photosensory flavoprotein in *Arabidopsis thaliana* (1) was identified in this organism (131).

STRUCTURE AND FUNCTION OF SR-HTR COMPLEXES

The primary structures of a number of sensory rhodopsins have been determined and analysed by comparison with the ion-pumping rhodopsins. Aspects of the SRs that have been studied include their photochemistry, the mechanisms

³The subscript indicates the wavelength of maximal absorption in nanometers.

involved in their color regulation, and the identification of photointermediates that function as signaling states. The Htr proteins functioning as signal transducers for the SRs have been identified and their genes have been cloned, revealing functionally informative similarities with the chemotaxis transducers from *E. coli* and other eubacteria.

Structure of Sensory Rhodopsins

In 1989 the *sopI* gene encoding the SRI apoprotein (sensory opsin I) was cloned from *H. salinarum* (15) using amino acid sequence information obtained from the purified protein (121). A second *sopI* sequence was obtained from *Halobacterium* sp. strain SG1 by low stringency heterologous hybridization (132). The gene encoding an SRII apoprotein was obtained from *Natronobacterium pharaonis* (*psopII*) using a similar strategy, and from *Haloarcula vallismortis* (*vsopI*) by PCR (126). *H. salinarum sopII* was obtained in a comprehensive cloning effort of the transducer gene family in this organism, because of its position adjacent to the *htrII* transducer gene (173, 174). Sequence information on the cloned SRs and Htrs is given in Figures 2 and 3.

The gene-predicted sequences of these sensory rhodopsins indicate hydrophobic proteins with seven transmembrane segments. Their crystal structures have not yet been reported, but cryoelectron microscopy of two-dimensional crystals of BR has produced a three-dimensional structure of this membrane protein at near-atomic resolution (37). The BR structure provides a good first approximation to the structures of SRs, because the transmembrane helices can be aligned without gaps while preserving the positions of residues in the highly conserved retinal binding cavity (44). The alignment of the available SR sequences is shown in Figure 2.

The retinal binding Lys in helix *G* and residues lining the retinal binding pocket are highly conserved in BR, HR, and the sensory rhodopsins. The structure of the chromophores in sensory rhodopsins has been examined by retinal extraction, reconstitution with retinal isomers, and resonance Raman spectroscopy (31, 40, 52, 118, 141). The chromophores all contain a protonated Schiff base linkage at the attachment site of the all-*trans* isomer of retinal. The functional cycles of these pigments involve the photoisomerization of the retinal from all-*trans* to 13-*cis*. However, a difference in the isomer specificity of the unphotolyzed pigments has become evident through binding studies using retinal isomers and retinal analogues. The functional photoreactions of both BR and SRI entail light-induced isomerization of all-*trans* retinal to 13-*cis*. The BR apoprotein, Bop, forms pigments with retinal, added as either the all-*trans* or 13-*cis* isomer, and in the dark the apoprotein catalyzes the isomerization in its chromophore into a mixture of all-*trans* and 13-*cis* isomers, the latter accompanied by isomerization about the C=N bond as well (26). In contrast,

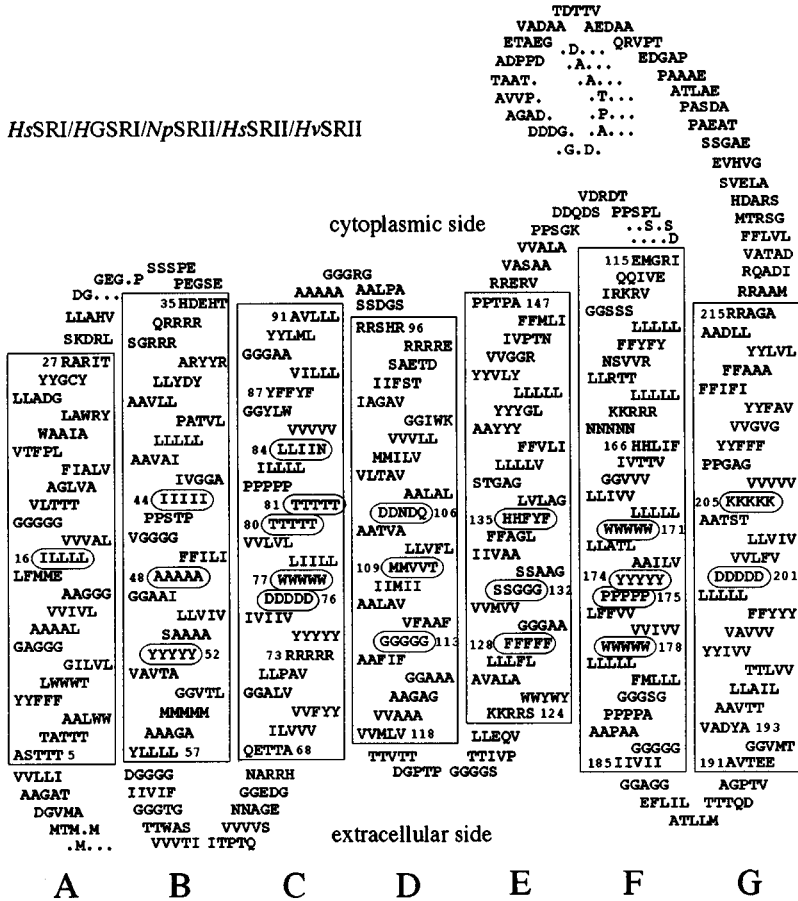


Figure 2 Alignment of the five archaeal sensory rhodopsins of known sequence in a two-dimensional folding topology. Hydropathy analysis of the primary sequences indicates the presence of seven transmembrane α -helices (designated A through G). The helix boundaries have been drawn based on those of BR (37). Residues corresponding to BR residues forming the retinal binding pocket are circled. Depicted sequences are for *H. salinarum* SRI (15), *H. sp.* SG1 (132), *N. pharaonis* SRII (126), *H. salinarum* SRII (174), *H. vallismortis* SRII (126), from left to right, respectively. Numbering corresponds to *H. salinarum* SRI residues.

sensory rhodopsin binding pockets compared to those of BR and HR (6, 48, 49, 163, 170). This property may be physiologically relevant in avoiding thermal noise (143).

Color Regulation

Complex interactions between the retinal chromophore and its protein environment cause the absorption maxima of the rhodopsins to deviate strongly from the absorption maximum of a protonated Schiff base model compound in methanol in the presence of Cl^- . The shift to longer wavelength caused by protein-chromophore interactions expressed as a wavenumber difference has been designated the opsin shift (94). As discussed above, the position of the absorption maxima of SRI, SRII and the SRI photointermediate S_{373} are of importance to the cells' physiology, since they determine the spectral regions of phototactic accumulation and avoidance. Below we present the data available on the mechanism of the opsin shifts in SRI and SRII.

The opsin shift has been investigated in detail for BR (4, 23, 51, 83, 166) and three contributing factors have been identified: (a) the positive charge on the protonated Schiff base is only *weakly* stabilized by a complex counterion provided by the protein environment, (b) the protein forces the conformation of the $\text{C}_5\text{—C}_6$ single bond in the retinal to be *6s-trans* allowing ring/chain coplanarity, and (c) a third factor is evident from a chromophore analogue in which the other two factors are eliminated (166). While it has been suggested that the weak counterion accounts for two-thirds of the opsin shift and the coplanarization for most of the rest (4, 51, 83), a recent study indicates that the contribution of the third factor is at least 40% (166). The physical basis of this important third factor is not yet clear. Two possibilities involving permanent or induced protein dipoles have been suggested (166) based on the observation that photoexcitation results in polarization of the retinal (84): (a) fixed polar groups around the polyene chain of retinal may stabilize the excited state or destabilize the groundstate of the chromophore; and (b) polarizable protein side chains may cause excited state stabilization. Support for such dipole effects is provided by findings that hydroxyl groups play a key role in wavelength regulation in human cone pigments (7, 68, 88).

The nature of the counterion has been investigated in retinylidene proteins because of its role in the opsin shift as well as in Schiff base deprotonation, an important event for proton pumping by BR and signaling (discussed below) by archaeal sensory rhodopsins and human rod rhodopsin. The counterion in BR_{568} is complex and involves a quadrupole (22) consisting of the positive charges of the protonated Schiff base and Arg82 and the negative charges of Asp85 and Asp212 (25, 74, 75). These residues are conserved in all SRI and SRII sequences (Arg 73, Asp 76, and Asp 201 in *HsSRI*) (Figure 2).

BR at low pH ($pK \sim 3.0$) exhibits a shift in its absorption maximum from 568 nm to 605 nm (56). A similar λ_{\max} is seen at neutral pH in D85N,⁴ and protonation of Asp85 is responsible for this purple to blue acid transition (147). The protonation state of the homologous residue Asp76 in SRI is responsible for a similar transition from 587 nm to 552 nm at alkaline pH (pK 8.5 in complex with HtrI, 7.2 in the absence of HtrI), as proven by UV-Vis and FTIR spectroscopy of isolated wild-type SRI and the D76N mutant at various pH values (17, 101, 110, 111). The purple BR₅₆₈ is the physiological functional (proton pumping) form of BR, while the blue SR₅₈₇ is the functional (sensory signaling) form of SRI.

The identical shift of 1080 cm^{-1} due to the protonation of Asp85 and Asp76 in BR and SRI, respectively, presumably results from weakening of the counterion [factor (*a*) above]. Resonance Raman measurements comparing the blue form SR₅₈₇ (protonated Asp76) and the purple form BR₅₆₈ (deprotonated Asp85) show a lower value of the Schiff base C=N stretching frequency in the former and its smaller shift upon deuteration, providing a direct indication for a weaker counterion (31).

Reconstitution of SRI apoprotein using 6-*s-cis*- and 6-*s-trans*-locked retinal analogues (9) indicates a 6-*s-trans* and co-planar conformation in SRI as in BR [factor (*b*)]. A faster rate of pigment formation is observed with the 6-*s-trans*-locked retinal than with native retinal, indicating that ring/chain coplanarization is a rate-limiting step in reconstitution. The similar effects of 24 retinal analogues on the absorption maxima of BR and SRI (163) further support that the mechanism of wavelength regulation in SRI and BR is very similar.

The absorption spectrum of SRII from *H. salinarum* displays two features that are different from the spectra of the other archaeal rhodopsins. First, its maximum is positioned at 487 nm, blue-shifted with respect to BR₅₆₈, HR₅₇₈, and SR₅₈₇ (153). The same is true for the absorption maximum of pSRII (500 nm; 119). In this respect, SRII is similar to the scotopic visual pigment ($\lambda_{\max} = 498$ nm) found in human eyes, which is also tuned to the energy peak of the solar spectrum. Second, the absorption spectrum of SRII shows vibrational fine structure at physiological temperatures (153).

The mechanism of color regulation in SRII was examined using a wide range of chromophore analogues (153). It was found that ring/chain co-planarization in the 6-*s-trans* conformation is sufficient to explain nearly all of the opsin shift of 2200 cm^{-1} in SRII. Thus, the relatively small opsin shift in SRII apparently results from its relatively strong counterion and the lack of a significant

⁴Residues are designated by the three-letter abbreviations for the amino acids, while proteins containing specific substitutions are designated using the standard one-letter code for the amino acids. Thus D76N signifies a derivative of SRI in which Asp76 is replaced by Asn.

contribution from factor (c) discussed above. These two factors may lead to a reduction in the inhomogeneous broadening of the absorbance bands, revealing the underlying vibrational fine-structure in SRII (153).

The residues forming the counterion in BR (Arg82, Asp85, and Asp212) are all conserved in the SRIIs (126, 174). However, a difference of SRII from all other archaeal rhodopsins is the change of Met118 (BR number) to Thr or Val. This methionine forms a cap on the pocket for the β -ionone ring in BR (37), and may be involved in ring/chain coplanarization (83), a notion that is supported by the blue-shift of the absorption maximum of the M118A mutant BR to 478 nm (light-adapted) without development of fine structure (36). In addition, an adjacent residue on the same helix, Asp115, present in all other archaeal rhodopsins, is found in SRII from *H. salinarium* but not in the other SRII proteins.

Photochemical Reaction Cycle Intermediates

Absorption of a photon by the unphotolyzed state of SRI, SR₅₈₇, initiates a cyclic chain of transitions (photocycle) containing three thermal intermediate states, SR₅₈₇ \rightarrow S₆₁₀ \rightarrow S₅₆₀ \rightarrow S₃₇₃ \rightarrow SR₅₈₇ (141).⁵ The only long-lived intermediate in the SRI photocycle is S₃₇₃ [800 ms in isolated membranes and 1.2 seconds in energized cells at 23°C (73)]. Since its rate of formation is 3000 times higher than its decay (Figure 4), S₃₇₃ can attain physiologically active concentrations after a flash of light or in the photostationary state established by continuous orange illumination. Near-UV light photoreconverts S₃₇₃ ten times more rapidly to SR₅₈₇ via the intermediate S₅₁₀^b. In the cell, the orange and near-UV light photoreactions of SR₅₈₇ and S₃₇₃ generate attractant and repellent responses, respectively. The activation of as few as one to two S₃₇₃ molecules is sufficient to elicit a repellent response (140). Hence, the interconversion of the two receptor forms by light (photochromicity) and the opposite cellular signals associated with these photoreactions provide the cell with a simple yet highly effective color-discriminating capability with exquisite sensitivity.

The photocycles of SRII (Figure 4) and pSRII have been studied in intact membranes and in detergent at physiological and at cryogenic temperatures. At room temperature the SRII and pSRII photocycles have half-lives around 350 milliseconds. Using the nomenclature applied to the analogous species in BR, K-, M- and O-like intermediates have been observed for both pigments at room temperature (90, 119, 130, 156, 158), but an L-like intermediate has been detected only for pSRII (53). Additional species have been observed after irradiation of SRII and pSRII at cryogenic temperatures (47, 54).

⁵The intermediates, S₆₁₀, S₅₆₀, S₃₇₃ correspond in absorption spectra and position in the cycle to the BR intermediates K₆₀₀, L₅₅₀, and M₄₁₂, and are sometimes referred to as SRI K, L, and M.

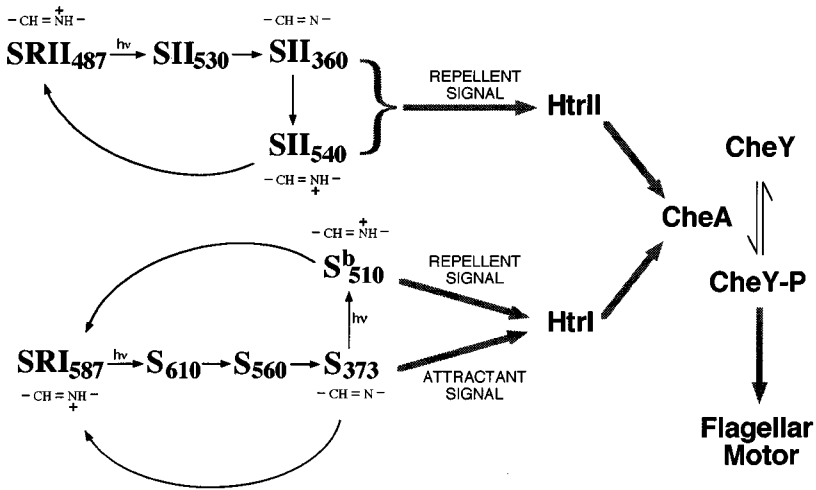


Figure 4 Photochemical reaction cycles of *H. salinarum* sensory rhodopsins I and II and their coupling to the flagellar motor. Arrows with $h\nu$ indicate light reactions. Subscripts are the wavelength maxima observed for the pigments or calculated for their photointermediates from flash photolysis data. The state of protonation of the Schiff base is indicated. Approximate first order half-lives at room temperature for SRI intermediates S_{610} , S_{560} , S_{373} , and S_{510}^b are 90 μ s, 270 μ s, 800 ms, and 80 ms, respectively, and for SII $_{530}$, SII $_{360}$, and SII $_{540}$, 160 μ s, 120 ms, and 330 ms, respectively. The indicated signaling states (see text) in each photocycle transmit signals through HtrI and HtrII to CheA. CheA controls the extent of phosphorylation of CheY, and phosphorylated CheY induces swimming reversals.

Identification of Receptor Signaling States

Intermediate lifetimes in the SR photocycles can be quantitated by kinetic absorption flash spectroscopy and modified by replacement of retinal with chromophore analogues *in vivo* using retinal-deficient strains of *H. salinarum*. The motility responses resulting from the excitation of the modified SRs have been quantitated by computerized cell tracking and motion analysis (151). In an early study, an acyclic retinal analogue decreased the photocycling rate, and increased phototactic sensitivity, indicating that signaling is governed by the lifetime of a photocycle intermediate(s) rather than by the frequency of photocycling (87). This result provided an approach for the *in vivo* determination of spectral states producing phototaxis signals. The photocycle is measured for each modified SR, and concentrations of photocycle intermediates integrated over time are calculated. These values are correlated with the sensitivity of the cells containing the modified SR derived from fluence-response curves obtained by cell tracking. In the case of SRI the attractant response to orange light is proportional to the concentration of the unprotonated Schiff base species in

the photocycle, S_{373} , indicating that this intermediate is the attractant signaling state (165).

The intermediate S_{373} is photoreactive and its excitation results in a repellent response by the cells. This repellent response to near-UV light is more sensitive than the attractant response to orange light and is proportional to the concentration of S_{373} in a photostationary state generated by continuous orange light illumination (140). Therefore, S_{373} plays a dual role as orange attractant signaling state and near-UV repellent receptor. Since either a decrease in orange light or an increase in near-UV light in an orange background results in a reduction of S_{373} levels, the sensitive near-UV response has been suggested to be caused by the rapid disappearance of the attractant signaling state (77). However, simultaneous stimulation with orange and near-UV light, although it results in a net increase in S_{373} concentration, produces a strong repellent response (140). Therefore, a new signaling state with a repellent effect must be produced by S_{373} photo-excitation. This conclusion has been confirmed genetically by isolation of an SRI mutant receptor (D201N) that does not produce attractant signals to orange light, but still mediates wild-type near-UV repellent responses to S_{373} excitation (101). Therefore, models in which only one signaling state is proposed to mediate both one-photon and two-photon responses are excluded. Figure 4 shows a model in which two distinct signaling states are formed by photo-excitation of SR_{587} and S_{373} . We assume that S_{510}^b is the repellent signaling state, since it is the only intermediate observed and its lifetime is compatible with this function.

Although three distinct states (SR_{587} and the attractant and repellent signaling states) are necessary to explain the photoresponses, these three states may be generated by shuttling between only two structurally distinct conformations of SRI. A model involving only two SRI conformations is accomplished by assuming that SR_{587} is an equilibrium mixture of the two conformations and that this equilibrium is shifted in opposite directions in the S_{373} and S_{510}^b states (142).

The method of *in vivo* determination of signaling states using retinal analogues that differentially affect the lifetimes of photocycle intermediates has also been applied to SRII (168). As was found for SRI, signaling efficiency correlates with photocycle duration. The sensitivity of the cells to the repellent effect of blue light is proportional to the lifetime of the S_{373} -like intermediate (with deprotonated Schiff base) of SRII. However, studies with one analogue indicated that the signaling state persists through the next intermediate, which has a protonated Schiff base (168).

Structure of Sensory Rhodopsin Transducers

The second protein in the SRI signaling pathway was identified by mutant analysis (134, 136). Based on its genetic association with SRI and its reversible

carboxymethylation, which is characteristic of eubacterial chemotaxis transducers (43, 105, 144, 149), the protein was proposed to function as a halobacterial transducer for SRI, relaying signals from the receptor to cytoplasmic components controlling the flagellar motor. This protein, now called HtrI, was isolated, partially sequenced, and the information used to identify and clone its gene, *htrI* (172). Like the *E. coli* transducers (methyl-accepting chemotaxis proteins or MCPs), the HtrI protein contains two transmembrane helices and a strongly conserved cytoplasmic region involved in binding of a histidine kinase (see Figures 1 and 3), and flanking regions containing carboxymethylation sites.

Compelling evidence has accumulated confirming the proposed role of HtrI as an SRI transducer. The *htrI* gene and the *sopI* gene encoding the SRI apoprotein are part of an operon under control of a single promoter (30, 172). Expression of the *htrI-sopI* pair restores phototaxis in a mutant containing a deletion in the *htrI-sopI* region (30, 171). The most definitive genetic evidence is that deletion of the region encoding the methylation and signaling domain of HtrI, although not affecting the proper folding and membrane association of the shortened protein, prevents restoration of SRI phototaxis (171). Furthermore, biochemical and spectroscopic evidence shows that SRI and HtrI are physically associated in the membrane (see below). Of practical importance to mutagenesis studies, cotranscription of *htrI* and *sopI* is not required for their functional association, because *htrI* chromosomally expressed from its native promoter and *sopI* expressed from a plasmid or from the *bop* locus on the chromosome produce an active complex (29, 61).

After *htrI* was cloned, a family of related genes was identified in halobacteria. The *htrI* gene from *H. vallismortis* was cloned and the predicted protein sequence found to be 57% identical to *H. salinarum* HtrI (57). The first *htrII* genes were identified in *H. vallismortis* and *N. pharaonis* (126), and *htrII* from *H. salinarum* was cloned recently (174), defining a second class of phototaxis transducers. As for *htrI* from *H. salinarum*, these four *htr* genes are positioned immediately upstream of *sop* genes.

Hydropathy analysis and alignment of these five Htr sequences with the *E. coli* chemotaxis transducers reveal features shared by all (Figure 3). They each have two transmembrane helices (TM1 and TM2), which in the case of the *E. coli* aspartate receptor Tar dimerize into a four-helix bundle (89). Two regions of conservation can be identified: (a) a strongly conserved (172) region of approximately 60 residues, generally referred to as the *signaling domain* (43, 105, 144, 149), implicated in binding the histidine kinase (CheA; 113) that controls the flagellar motor. The signaling domain is flanked by more weakly conserved methylation sites. And (b) a region of weak but converging homology contained within approximately 40 residues at the cytoplasmic end of TM2 (within the region called the linker segment in eubacterial MCPs; 5).

Mutagenesis studies have revealed the latter region to be important in the interaction between SRI and HtrI (55). For reasons discussed below we refer to this region as the *stimulus relay domain*.

The first transmembrane helix TM1 is located close to the N-terminal end in all cases (Figure 3). The position of TM2 is variable. In each of the *E. coli* transducers TM2 is found approximately 150 residues beyond TM1, defining a periplasmic ligand-binding domain (89). In HtrII from *H. salinarum* TM2 is found approximately 250 residues beyond TM1, defining a large periplasmic domain of unknown function. The *N. pharaonis* HtrII differs, displaying a periplasmic domain of only 18 residues. Also in the two known HtrI proteins the TM2 sequence is adjacent to that of TM1 and there is little or no periplasmic domain.

The precise membrane boundaries of TM1 and TM2 are not known. Therefore, the assignment shown in Figure 3 should be considered approximate. In particular, it is unclear whether the functionally important residue Glu56 in *H. salinarum* HtrI (see below) is embedded in the membrane or located in the cytoplasm near the membrane surface.

A number of results indicate a role of the region (stimulus relay domain), within approximately 40 residues of the cytoplasmic end of TM2, in the relay of signals from photostimulation of SRI to HtrI: (a) Seven residues in this region in *H. salinarum* HtrI (Glu56 to Glu108) influence the lifetime of the signaling state S_{373} (Figure 5B; 55). (b) Residues 1–147 of HtrI, which include the transmembrane helices and this region, are sufficient to confer a wild-type phenotype to the SRI photocycle, which is greatly altered when HtrI is removed (106). (c) Suppressors that restore attractant signaling to the E56Q HtrI and D201N SRI mutants are found in this region (K-H Jung and JL Spudich, unpublished results).

The stimulus relay domain of HtrI is well conserved among Htr proteins and contains nine residues shared by nearly all *E. coli*, *Salmonella typhimurium*, *Bacillus subtilis*, and *Enterobacter aerogenes* MCPs (Figure 3). In studies of heterodimers of Tar in which one monomer is full length and the other is progressively deleted from the cytoplasmic end, it was found that this domain cannot be removed without loss of chemotaxis (34, 155). Disulfide locking experiments (20) and mutagenesis (19) of *E. coli* Tar implicate movement of the adjacent TM2 in transmission of the stimulus (21). The region homologous to the stimulus relay domain of HtrI has been suggested to be involved in transfer of the signal between the two parts of the fusion proteins Tar-EnvZ and Trg-EnvZ (10). Such a region is not present in the *H. salinarum* transducers HtA and HtB (173), nor in FrzCD from *Myxococcus xanthus* (86), all transducers that lack transmembrane segments. These results implicate the domain in stimulus relay from the membrane to the cytoplasm in both Archaea and Eubacteria.

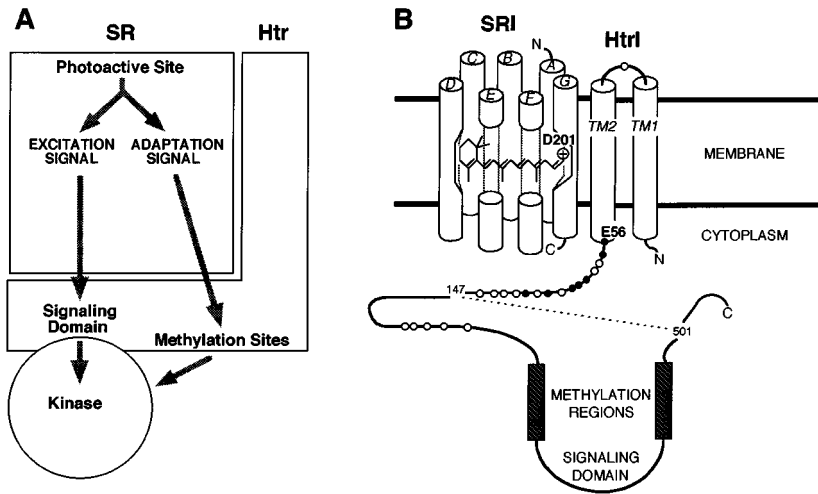


Figure 5 Signal relay from receptor to transducer. (A) Each attractant and repellent signal indicated in Figure 4 consists of two component signals relayed to the Htr protein: an excitation signal from SRI or SRII affecting kinase activity and an adaptation signal affecting transducer methylatability, which after a delay counterbalances the excitation signal effect on the kinase. (B) Regions of HtrI modulating SRI photocycle kinetics and signaling function. The N-terminal 147 residues of HtrI are sufficient to confer pH-insensitivity to the SRI photocycle (106). The HtrI residues R70, R84, D86, E87, R99, and E108 (filled circles) modulate the SRI photocycle (55). Open circles indicate the location of mutations not affecting signaling or photochemistry. The D201N mutation in SRI and E56Q mutation in HtrI lead to the inverted signaling phenotype (see text).

In eubacterial chemoreceptors and sensor kinases such as EnvZ a predicted amphipathic α -helix occurs immediately after TM2 (127, 128). A similar amphipathic sequence (AS in Figure 3) appears to be present in the Htr proteins (residues 60–73 in HtrI). The AS is involved in membrane insertion and has been suggested also to be involved in dimerization (127). This suggestion is in line with results of disulfide crosslinking of the HtrI mutant I64C, which shows quantitative crosslinking of HtrI dimers following oxidation (X-N Zhang and JL Spudich, unpublished results). A helix-turn-helix-turn-helix motif spanning the AS and stimulus relay domain is predicted by the Chou and Fasman algorithm in all of the transducers.

The highly conserved signaling domain of about 60 residues was identified originally in the *E. coli* transducers and has been characterized by genetic and biochemical studies (43, 105, 144, 149). This region binds the CheA kinase tightly and modulates its activity during signaling. Binding of a second protein, CheW, is required for this process. Signaling domains and associated CheA

proteins are widespread in chemotaxis systems in Eubacteria. Sequence analysis of HtrI showed that the signaling domain is also present in Archaea (172) and the gene encoding the CheA histidine kinase has been cloned from *H. salinarum* (113). An oligonucleotide probe to the region encoding the signaling domain, which is the most conserved region in all transducer genes, enabled the cloning of a family of 13 transducer proteins from *H. salinarum* including HtrI and II (173). In the most highly conserved part of the signaling domain, 28 out of 40 residues are identical in nearly all known transducers across the Eubacteria and Archaea.

Multiple methylation sites in the *E. coli* transducers have been identified in regions flanking the signaling domain. The level of sequence conservation of these regions is considerably lower than that of the signaling domain. Sequence alignment has revealed candidate methylation sites in HtrI (172) and the other transducers (126, 173) that have not been demonstrated experimentally.

SRI: STAGES IN SIGNALING

Phototaxis signaling by SRI involves the propagation of local changes induced by retinal photoisomerization to global changes in the SRI-HtrI complex. The balancing effect of activation and adaptation results in a transient signal carried by protein phosphorylation to the flagellar motor.

From Photon Absorption to Signaling State

Photoisomerization of the chromophore from all-*trans* to 13-*cis* initiates all subsequent dark transitions leading to signaling. In rhodopsin and BR the isomerization process is ultra-fast, being completed in 200 fs and 3 ps, respectively (82, 125, 161). In SRI the isomerization and consequent formation of the first intermediate S_{610} have not been kinetically resolved, but are expected to occur on a similar time scale. The necessity for isomerization is indicated by reconstitution experiments with SRI and SRII in which 13-*trans*-locked retinal analogues prevent the formation of S_{373} and block all phototaxis responses (167).

Two lines of evidence indicate that the retinal is highly sterically constrained by the binding pocket of SRI. First, it was reported that the first photointermediate S_{610} cannot be trapped at any temperature (220 to 80 K; 6). In all other retinylidene proteins studied the early photointermediates can be trapped at low temperatures. Such trapping is anticipated, since the absorption of a photon is expected to result in retinal isomerization, regardless of the freezing of protein motions. Therefore, protein vibrational motions appear to be required for the formation of S_{610} . These results have been interpreted in terms of an energy barrier on the excited state surface caused by interactions with side chains that

resist the isomerization (6). This interpretation is supported by a flash photolysis study (10- μ s resolution) of SRI at low temperatures, which showed that the flash-induced yield of S_{610} decreases below 220 K and reaches zero at 100 K, while in BR the yield of formation of the corresponding K intermediate is independent of temperature (170). Second, introduction of bulky substituents on the retinal polyene chain greatly retards or blocks the final step of chromophore binding to the apoprotein of SRI, whereas the same analogues exhibit little or no effect on binding to BR apoprotein (170). These results indicate a close interaction between the all-*trans* retinal and the SRI apoprotein.

A crucial site of interaction between the retinal and the protein has been revealed in studies of the photochemistry of SRI pigments reconstituted with various analogues. An intact β -ionone ring is not necessary for the coupling of retinal isomerization to protein conformational changes as most of it can be removed without loss of function (169). However, the 13-methyl group on the polyene chain functions as an essential steric trigger in formation of the signaling state S_{373} : 13-desmethyl retinal forms a pigment with SRI apoprotein with a nearly normal absorption spectrum, yet no flash-induced S_{373} is detected (163). Also in bovine rod rhodopsin, a polyene-methyl steric trigger has been identified; in this case it is the steric interaction between the protein and the retinal 9-methyl group that is crucial for the formation of the S_{373} -like signaling state metarhodopsin-II₃₈₀ (33). Since in rhodopsin the photoisomerization of the 11-12 instead of the 13-14 double bond occurs, a shared characteristic of these two steric triggers is that the nearest methyl group between the photoisomerizing double bond and the ring is used. Notably, in the 13-desmethyl SRI the formation of S_{610} is blocked according to flash photolysis measurements with 10- μ s time resolution (170), implying that interaction between a protein residue and the 13-methyl group of the retinal is required to overcome the energy barrier for isomerization observed at low temperature. This barrier could be overcome if isomerization-induced movement of the 13-methyl group would induce movement in the protein necessary to accommodate the 13-*cis* configuration. Further evidence for interaction at this site is that the rate of pigment formation from 13-ethyl retinal and SRI apoprotein is reduced 30-fold, whereas 13-ethyl retinal forms a pigment with BR apoprotein with a rate similar to that of native retinal (170).

Protein structural changes are presumably responsible for the thermal formation of S_{560} from S_{610} . This process is much slower (90 μ sec) than the corresponding steps in BR (K \rightarrow L, \sim 1 μ sec) or rhodopsin (batho to lumirhodopsin, \sim 0.1 μ sec). Resonance Raman measurements show that in SR₅₈₇ the retinylidene Schiff base is protonated (31) and in S_{373} it is unprotonated (40). The absorption maxima indicate that the deprotonation occurs during the conversion of S_{560} to S_{373} . FTIR light-dark difference absorption spectroscopy reveals

structural changes in the protein backbone and in the environments of unidentified residues including carboxylates upon formation of S_{373} from SR_{587} (18).

Stimulus Relay from the Signaling State to HtrI

The unphotolyzed SRI, SR_{587} (designated SRI_{587} in Figure 4 to distinguish it from $SRII$), forms a tight molecular complex with HtrI that persists throughout the photocycle. Therefore, unlike signaling from visual rhodopsin to transducin, stimulus relay from the signaling states of SRI to HtrI does not involve association/dissociation of the two proteins, but rather structural changes within the complex. The evidence for the stable complexation of SRI and HtrI derives from several lines of experimentation: (a) the molecules co-purify in SRI affinity chromatography (EN Spudich, P Dag, and JL Spudich, unpublished results), (b) transfer of retinal from SRI specifically to HtrI during treatment of native membranes with a reducing agent suggests proximity (134), and (c) HtrI influences various properties of SRI both in its SR_{587} and S_{373} states. This latter point is based on comparative studies (see below) that used wild-type membrane preparations and membranes either lacking HtrI or containing mutant forms of HtrI.

The presence of HtrI partially shields the chromophore in the unphotolyzed state SR_{587} from attack by hydroxylamine. In addition, the apparent pK_a of the Schiff base is above 12 in the presence of HtrI and 9.5 in its absence (164). Also the pK_a of Asp76, the protonation state of which can be monitored by the blue to purple transition, is shifted (from 7.2 to 8.5) by the presence of HtrI (17, 101, 111).

The above effects are those evident in the dark. The effects of HtrI on events during the photocycle were first detected by S_{373} decay measurements (135). These effects were interpreted as resulting from a physical coupling of HtrI to SRI that modulates proton transfer steps in the receptor. The formation and decay of S_{373} involve deprotonation and reprotonation of the Schiff base in SRI. In the absence of HtrI these proton transfers result in light-driven electrogenic pumping of protons across the membrane (17) when SRI is in its purple form. In contrast, in SRI complexed with HtrI these proton transfer reactions occur entirely within the membrane, because no changes in proton concentration are detected in the medium and the reactions are independent of external pH (99). Genetic removal of HtrI causes reprotonation of the Schiff base (i.e. S_{373} decay) to become highly pH dependent (135), and transient stoichiometric proton release is detected during the photocycle (100). The protonation kinetics are first order and the rate constant is proportional to external proton concentration. The slope of this pH dependence is significantly less than one (0.36 in Reference 135), suggesting a complex coupling of proton transfer events in SRI to the bulk pH (39). When HtrI is present in sub-stoichiometric amounts, both

pH-independent (HtrI-complexed) and pH-dependent (HtrI-free) photocycling SRI species are observed (59, 100), as would be expected from a stable complexation of a fraction of the SRI molecules with the available HtrI. The binding of HtrI to SRI also alters the temperature dependence of S_{373} decay (164).

The rate of flash-induced deprotonation is greatly affected by HtrI binding,⁶ and the yield (135) of S_{373} is larger in the complex because of the suppression of thermal branching reactions from the S_{610} and S_{560} states to SR_{587} (143). Also in bovine rod rhodopsin an increase in flash-yield of the deprotonated Schiff base species (Meta-II₃₈₀) is observed upon binding of its transducer (the G-protein transducin) (108). In free SRI in membranes as well as in purified detergent-solubilized SRI (62) the formation of S_{373} occurs in μs times in the purple form [$t_{1/2} = 10 \mu s$ at 18°C (EN Spudich, P Dag, and JL Spudich, unpublished results); $t_{1/2} = 3$ to $5 \mu s$ at 23°C (I Szundi and RA Bogomolni, unpublished results)], in which Asp76 is the proton acceptor (111). In the blue form of free SRI Asp76 is not ionized and the rate of S_{373} formation is reduced 1000-fold ($t_{1/2} \geq 10$ ms; EN Spudich, P Dag, and JL Spudich, unpublished results). In the SRI-HtrI complex (blue form, measured at pH values 5 to 8 in membranes and in purified complex) neither the fast ($10 \mu s$) nor the slow (≥ 10 ms) rate is detected; rather a first order rate of $300 \mu s$ is observed (EN Spudich, P Dag, and JL Spudich, unpublished results). Note that in the complex (blue form) Asp76 is not available as a proton acceptor, and therefore HtrI interaction *facilitates* deprotonation of the Schiff base in this state of the protein, since without HtrI the blue form exhibits the ≥ 10 ms rate.

The initial demonstration of single photon-driven proton pumping by HtrI-free SRI used pH and TTP⁺ electrodes and membrane envelope vesicles (17). Measurements at high light intensities with pH electrodes have been applied to whole cells and have led to the identification of an additional novel proton translocation process interpreted as a two-photon cycling between two thermally metastable intermediates of the SRI photocycle, S_{510}^b and S_{373} (41). A similar process has also been observed in envelope vesicles (150). The presence of both one- and two-photon pumping modes in SRI was confirmed by measurements with *H. salinarum* membranes attached to black lipid membranes (BLM; 39). In this study proton pumping was observed by membranes containing wild-type SRI-HtrI complex, although in previous work, HtrI was reported to block proton release (100) and pumping (17). Since the BLM method is more sensitive, although not quantifiable in terms of protein-specific activity, it is possible that HtrI reduces pumping by SRI to a level below the detection limit of

⁶An identical rate of deprotonation of $380 \mu s$ in both the SRI-HtrI complex and the purple form of free SRI has been reported (39), at variance with the difference in these rates reported here. This variance may be the result of an overestimation of the time resolution in the published study.

the other methods (~5%). Alternatively, a small fraction of HtrI-free SRI may be present in the membranes, and responsible for the BLM signals. Supporting this latter option are the flash photolysis data (39) of complex-containing membranes used for the BLM measurements, that show a slow (≥ 10 ms) phase in S_{373} formation with an amplitude of 2–5% which vanishes above pH 7 (i.e. at a pH where Asp76 becomes ionized in free SRI), as would be expected for HtrI-free but not for HtrI-complexed SRI.

The region of HtrI necessary for conferring pH-independence to the S_{373} decay process has been localized by deletion analysis to the N-terminal 147 residues containing the two transmembrane helices and the stimulus relay domain (106).⁷ Within this fragment, substitution with neutral amino acids either accelerates (Glu56, Asp86, Glu87, or Glu108) or retards (Arg70, Arg84, or Arg99) S_{373} decay (55). Opposite effects on the rate cancel in double mutants containing one replaced acidic and one replaced basic residue. The effect of substitution of Glu56 depends on the electronegativity of the residue introduced. These results indicate that electrostatic interactions of these residues with SRI or with other HtrI residues are involved in the coupling of HtrI to the SRI photoactive site.

A large effect of HtrI on the rotational diffusion rate of SRI and the angle of the chromophore with respect to the membrane plane has been observed by polarization anisotropy (RA Bogomolni, unpublished results). From the decay of the photoinduced dichroism generated by polarized laser light a rotational diffusion time of SRI in native membranes of about 200 μ s was obtained. HtrI-free SRI, however, exhibits a shorter rotation time (≤ 10 μ s). The 200 μ s time is significantly longer than that expected from a 25 kD membrane protein in a typical lipid bilayer environment but is comparable to the rotational times observed for small aggregates of HR or BR. Both BR and HR occur in aggregated or oligomeric states in the membrane, and strong evidence for this aggregation is the visible circular dichroism (CD) spectrum of the pigments which shows the typical negative-positive bands expected from exciton interaction between proximal retinal chromophores. In contrast, SRI in the native state yields a CD spectrum devoid of exciton coupling features (38). The 200 μ s correlation time would be consistent with an SRI molecule in a more massive complex in the membrane. In addition, from the residual of the anisotropy an approximately 5-degree tilt of the SRI chromophore appears to be induced by HtrI.

Analysis of these effects of HtrI on SRI in the context of our current understanding of the BR pumping mechanism has led to the following view: Like

⁷Deletion of a short region of the signaling domain in HtrI was reported to abolish interaction with SRI (58), whereas removal of the entire signaling domain and flanking regions were reported not to disrupt SRI-HtrI interaction (171). In the former case, the particular HtrI deletion construct may be impaired in folding or membrane insertion, explaining the HtrI-free properties of SRI.

BR, SRI contains both a cytoplasmic and extracellular channel capable of proton conduction. Alternate access of these channels to the Schiff base during the photocycle permits proton release and uptake on opposite sides of the membrane, leading to vectorial proton translocation. HtrI increases the pK_a of the gatekeeper for the extracellular channel, Asp76, thereby preventing it from accepting the Schiff base proton. Also, the cytoplasmic channel is blocked by the interaction with HtrI, although the mechanism is less clear. The stimulus relay domain may be involved, based on its location and properties. Either the proton movement or the structural changes during the switch in accessibility of the Schiff base (or both) may generate the receptor phototaxis signals (138).

The proton acceptor in the purple form of free SRI has been identified as Asp76 by FTIR difference absorption spectroscopy on wildtype and D76N mutant membranes (111). However, the fate of the proton after its release from the Schiff base during S_{373} formation in the complex is unclear. The proton acceptor is not Asp76, since it is already protonated in SR_{587} . The FTIR light-dark difference spectra display signals in the carboxylate region that indicate perturbation, but not protonation, of a carboxylate group (18, 110, 111), which suggests the involvement of some other group.

Transducer Activation and Adaptation: Two Signals

In the unstimulated state halobacteria spontaneously reverse their swimming direction approximately every 5 to 50 seconds. Photostimuli alter the behavior of the cells by modulating the reversal frequency. An abrupt increase in attractant (orange) light suppresses reversals (the *excitation* phase of the response). Afterward the cells regain their prestimulus reversal frequency (*adaptation*). Adaptation times of 3 to 20 sec have been measured, depending on the strength of the stimulus. An abrupt decrease in attractant light induces a transient increase in reversal frequency in a cell population. These responses to temporal changes in light intensity operate as the cells swim in regions of varying light intensity (spatial gradients). Therefore, in spatial gradients of orange light, the cells' swimming paths are prolonged as they swim up the gradient and shortened as they swim down the gradient, resulting in net migration toward higher intensities of orange light. Gradients of blue or near-UV light have the opposite effects on reversal probability and, therefore, repel the cells.

The behavioral physiology of phototaxis is understood from early visual cell tracking techniques and more recent computerized infrared video motion analysis (151). Also, a rapid population method for quantitating phototaxis accumulation and dispersion has been developed and applied to halobacteria (145; see also 97, 141, 143 for more details). Several mathematical models have been presented that account for various aspects of the response kinetics (70–72, 76, 78, 79, 93, 122, 123, 154) and an in-depth analysis of models for signal

transduction and motor switching in halobacteria has been conducted (107). Extensive single cell tracking experiments have been designed and performed to test such models and have made important contributions to the study of behavioral kinetics (63, 64; see 143 for a review).

Changes in light intensity and color result in shifts in the steady state concentrations of SRI signaling states. Attractant signaling states inhibit the histidine kinase and repellent signaling states activate it. Even when the change in concentration of a signaling state persists (after a step-up or step-down in light intensity), the swimming response is transient. The resetting of reversal probability (adaptation) is presumably accomplished by changing the extent of transducer methylation, where an increase or decrease in methylation leads to kinase activation or deactivation, respectively. This means that a change in signaling state concentration generates two opposing signals (see Figure 5), one responsible for the excitation phase of the response, and the other responsible for adaptation. The adaptation process precisely nullifies the excitation signal's effect on the kinase, as evidenced by the fact that the spontaneous reversal frequency is the same at different light intensities (141). This role of methylation was elucidated in studies of *E. coli* chemotaxis (43, 105, 144, 149) and this well-established paradigm appears to be applicable to halobacterial phototaxis based on the physiological (143), biochemical (2, 3, 134, 136), and genetic (113–115, 172) homology between the two systems. Also in bovine rod rhodopsin, photoexcitation of the receptor produces both excitation and adaptation signals, in this case involving the activation of the binding of the G-protein transducin and the activation of rhodopsin kinase, respectively. These two signals in rod rhodopsin have been biochemically separated at the level of the receptor: the former requires Schiff base deprotonation, while the latter does not (108).

Interplay between the excitation and adaptation signals produces four elemental transient responses (see Figure 6): (a) a *primary* response to an increase in S_{373} concentration by a step-up in orange light; (b) a *deadaptation* response to a decrease in S_{373} concentration by a step-down in orange light; (c) a *primary* response to an increase in S_{510}^b concentration by a step-up in near-UV light in an orange light background; and (d) a corresponding *deadaptation* response to a decrease in near-UV light. The primary responses are caused by the light-induced population of a signaling state, which causes a change in kinase activity. The deadaptation responses are caused by the removal of the signaling state and presumably the resulting transient existence of an inappropriate level of transducer methylation. The existence of deadaptation responses requires that the methylation level modulates kinase activity independent of the signaling state's effect on the kinase, as indicated in Figure 5, and that the signaling state affects two regions of the transducer: the signaling domain and the methylation region.

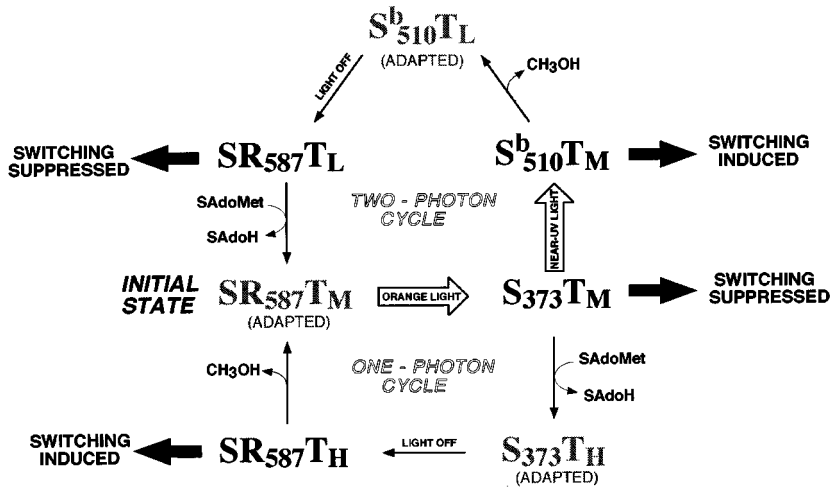


Figure 6 Phototaxis signaling by the SRI-HtrI complex. In the dark (initial state), SR₅₈₇ is complexed to HtrI transducer protein which has an intermediate level of methylation (T_{M(edium)}). *One-photon cycle*: A step-up in orange light results in the formation of S₃₇₃, which decreases CheA activity and therefore CheY phosphorylation, leading to a suppression of reversals (switching). Adaptation occurs via methylation of HtrI (T_{H(igh)}). A subsequent step-down in orange light (light off) results in the net reformation of SR₅₈₇, now complexed to a highly methylated HtrI. This state of the complex activates CheA and leads to an induction in reversal frequency, which is reset by the subsequent return of the methylation level of HtrI to the initial level. *Two-photon cycle*: A step-up in both orange and near-UV light causes accumulation of S₅₁₀^b, which activates CheA, leading to an increase in reversal frequency. Adaptation occurs via demethylation of HtrI (T_{L(ow)}). A subsequent step-down in orange/near-UV light (light off) results in the net formation of the SR₅₈₇/HtrI complex with a low methylation level, suppressing CheA activity and reversals. Methylation of HtrI returns the complex to its initial state and resets the reversal frequency.

Stimuli alter the methylatability of MCP transducers in *E. coli*, a substrate-directed effect in which an MCP is the substrate. In *E. coli* chemotaxis the rate of approach to the new substrate-directed level is aided by a feedback control of CheB carboxymethyl esterase activity by coupling its activity to CheA activity, accomplished by CheA phosphorylation of CheB (144, 149). Consequently, large increases and decreases of carboxymethyl turnover rate occur following repellent and attractant stimuli, respectively, in *E. coli*. Carboxymethylated transducers (2, 3, 45, 134, 136) and photo-stimulated increases in turnover rate of methyl groups are also observed in *H. salinarum* cells by methanol release studies (3, 95, 136, 148), indicating a similar feedback control by the kinase. However, in *H. salinarum* increases in methanol release follow both attractant and repellent stimuli. This lack of asymmetry may be explained by

coupling of kinase activity to both the methyltransferase and methyl-esterase activities. The CheB from *H. salinarum* contains a sequence motif for phosphorylation by CheA (115), while the methyltransferase gene has not been identified.

From Signaling Complex to the Flagellar Motor

Early cell tracking studies and mutant analysis established that an integrated signal from phototaxis and chemotaxis receptors modulates the flagellar motor switch. A cluster of genes designated *cheY*, *cheB*, *cheA* and *cheJ* has been cloned from *H. salinarum* (113–115). The first three genes are homologous to their counterparts in the *E. coli* chemotaxis system and it was shown that CheA has autophosphorylation activity and CheY stimulates its dephosphorylation, as expected from phosphotransfer to CheY (115). Deletion of either *cheA* or *cheY* results in a smooth swimming phenotype, as in *E. coli* (114). This observation fits the expectation from the *E. coli* paradigm that phospho-CheY causes swimming reversals upon binding to the flagellar motor switch in *H. salinarum*. The *cheJ* gene appears to be a new member of the *che* gene family, since it shows no obvious homology to other known *che* genes although it is involved in taxis as shown by the fact that its deletion results in partial inhibition of chemotactic swarming and of phototaxis (114). Homologs of the *E. coli* *cheR*, *cheW* and *cheZ* have not been identified. The interaction of CheY-P with the flagellar switch complex differs in *E. coli* and *H. salinarum*: It biases the *E. coli* flagellar motor to rotate clockwise (causing tumbles), whereas it induces a change in the direction of rotation (causing swimming reversals) regardless of the initial direction in *H. salinarum* (115).

An additional component has been proposed as part of the phototaxis signal transduction chain: fumarate (“switch factor”) binding protein (FBP; 81). The existence of FBP is inferred from biochemical experiments showing that (a) fumarate is released to the cytoplasm when reversal-inducing stimuli are delivered through SRI or SRII (80, 91); and (b) fumarate restores stimulus-induced reversals in a non-reversing mutant at the level of one or a few molecules per cell (81). Fumarate is required for switching the direction of flagellar rotation in cytoplasm-free envelopes of *E. coli* (8). It may act by lowering the activation energy for switching and may connect the bacterial metabolic state to tactic behavior (27).

SRII: RECENT PROGRESS

Light-induced difference FTIR spectroscopy on purified SRII from *N. pharaonis* indicates the protonation of a carboxylate during the formation of the S₃₇₃-like intermediate in the pSRII photocycle (27a, 117). The FTIR band caused by

this event in SRII is similar to that caused by Asp85 protonation in BR and by protonation of the corresponding Asp76 in the proton pumping form of SRI, a band which is missing in the sensory signaling form of SRI. The recent cloning of *htrII-sopII* gene pairs (126, 174) has made the SRII system amenable to analysis by genetic manipulation. The first site-specific mutagenesis work has led to the identification of Asp73 as the proton acceptor and Schiff base counterion in SRII from *H. salinarum* (EN Spudich, W Zhang, M Alam, JL Spudich, unpublished results), whereas in SRI the corresponding aspartyl residue remains neutral during phototaxis signaling. This difference could have significance for the opposite signals produced by Schiff base deprotonation in the two receptors (126).

The D73N mutation results in a shift in the SRII absorption spectrum from 487 nm to 514 nm, a red-shift of 1080 cm^{-1} , identical to that of the purple-to-blue transitions in BR and SRI that result from protonation of the homologous aspartates. The mutation also causes a loss of vibrational fine structure, indicating that the weakened counterion contributes to inhomogeneous broadening as discussed earlier in the section on color regulation. Coexpression of the genes encoding D73N and the SRII transducer HtrII in *H. salinarum* cells results in a threefold higher swimming reversal frequency in the dark than that from coexpression of native SRII and HtrII, and the D73N mutation causes demethylation of HtrII in the dark, indicating that D73N produces repellent signals in its unphotostimulated state (EN Spudich, W Zhang, M Alam, JL Spudich, unpublished results). Analogous constitutive signaling has been shown to be produced by the similar neutral residue substitution of the PSB counterion and proton acceptor Glu113 in human rhodopsin apoprotein (109).

Consistent with the activating effect of the D73N mutation in the dark, cells carrying this mutation exhibit a strongly reduced taxis response. Therefore, proton transfer is important for forming the signaling state, but some signal is generated without the transfer of the Schiff base proton to Asp73. This result is analogous to that obtained with visual pigments, in which proton transfer from the Schiff base to Glu113 is an important factor in stabilizing the G protein-activating state (109), stabilization to which other determinants also contribute significantly (28).

INVERTED SIGNALING

Mutagenesis studies on both SRI and HtrI have led to a recurring unusual mutant phenotype called *inverted signaling*, in which the cell produces a repellent response to normally attractant orange light (55, 101). The inverted mutant cells exhibit a wild type repellent response to near-UV light, genetically

separating the repellent and attractant signaling processes. The D201N SRI (101), E56Q HtrI (55), and several substitutions of His166 in SRI (X-N Zhang and JL Spudich, unpublished results) all result in this phenotype. Therefore, these residues appear to be essential for attractant signaling. Attempts to explain the unexpected conversion of the orange light into a repellent stimulus by single mutations has spawned new ideas on the signaling mechanism (see below).

As discussed above, any change in light intensity results in two signals, one activating and one suppressing the kinase. Normally, the kinetics of these two signals from a step-up in orange light is such that the excitational suppression of kinase activity precedes the compensating activation (adaptation). A possible explanation for the inverted response is that the mutations invert the kinetics of the excitation and adaptation signals.

Another approach to explaining the inverted signaling phenotype is based on the notion that the SRI-HtrI complex is poised in an equilibrium between two conformations, which is easily shifted towards one or the other conformation by single mutations. Two conformations of BR have been directly detected by cryoelectron microscopy (44, 146). An expansion of the cytoplasmic channel is observed during the BR₅₆₈ to M₄₁₂ photoconversion (corresponding to the SR₅₈₇ to S₃₇₃ photoconversion) and is implicated in the change of accessibility of the Schiff base from the extracellular membrane surface to the cytoplasmic membrane surface. The conformation with an open cytoplasmic channel can be reached in the dark by single mutations, as revealed by ion transport measurements (116). Light-induced shuttling between two such conformations evidently occurs in free SRI, since it is capable of proton transport (17), and the presence of these two conformations in the SRI-HtrI complex can explain attractant and repellent signaling, if one assumes that an equilibrium mixture of the two conformations with opposite effects on HtrI exists in the dark (142). This model provides a rationale for the blocking of the cytoplasmic channel of SRI by HtrI, since HtrI may monitor the state of SRI at this structurally active site. In addition, inverted signaling can now be rationalized in terms of mutation-induced shifts of the equilibria between the two conformations in the dark and in photoproducts (142).

Based on the conformational shuttling model the existence was predicted of suppressor mutations that restore the conformational equilibrium disturbed in the inverted signaling mutants. Such mutants would exhibit orange light-induced attractant responses, while an overcompensation by the suppressor mutation would eliminate the two-photon repellent response. Recently, both intragenic and extragenic suppressor mutations to D201N in SRI and E56Q in HtrI have been found in the complex which fulfill this prediction (K-H Jung and JL Spudich, unpublished results).

Lowering extracellular pH is another way to correct the inverted phenotype (55). This observation supports the notion that the coupling of SRI to HtrI involves electrostatic interactions, as was derived from the effects on the SRI photocycle kinetics of neutralization of acidic and basic residues in HtrI by site-specific mutagenesis (55).

PERSPECTIVES

The SR-Htr signaling complexes offer an opportunity for studying the biophysical chemistry of signal generation and relay, in order to elucidate fundamental principles of sensory transduction and more broadly the nature of dynamic interactions between membrane proteins. As reviewed here, many aspects of these complexes are being probed, from the photobiophysics of initial excitation of the receptors to the final output at the level of the flagellar motor switch. Structural features and their dynamics are beginning to be revealed by molecular spectroscopy, and information with near-atomic resolution is within reach by cryoelectron microscopy of the complexes. Study of the SR system benefits from the close similarities (*a*) between SRs and BR, one of the few membrane proteins undergoing extensive structure/function analysis at the atomic level, and (*b*) between Htrs and the *E. coli* Tar for which partial crystallographic and extensive genetic and biochemical information is available. At the functional level, the processes of receptor activation and signal relay in visual pigments and archaeal sensory rhodopsins have been mutually informative.

Future developments in unraveling the molecular mechanism of photosignaling by sensory rhodopsins are likely to involve the use of overexpressed components for *in vitro* studies on function and for crystallography on two-dimensional or three-dimensional lattices of the complex, and exploitation of the recently implemented molecular genetic tools in combination with selection methods for phototaxis and suppressor mutants to identify critical residues and domains and to dissect function.

ACKNOWLEDGMENTS

We thank Maqsdul Alam, Richard Henderson, K Peter Hofmann, and Janos Lanyi for providing us with information from their experiments prior to publication, and Walther Stoeckenius for critical reading of the manuscript. The authors' work on this topic was supported by National Institutes of Health grant R01 GM27750 (to JLS) and a fellowship of the Cancer Research Fund of the Damon Runyon-Walter Winchell Foundation (to WDH).

Visit the *Annual Reviews* home page at
<http://www.annurev.org>.

Literature Cited

- Ahmad M, Cashmore AR. 1993. HY4 gene of *A. thaliana* encodes a protein with characteristics of a blue-light photoreceptor. *Nature* 366:162–66
- Alam M, Hazelbauer GL. 1991. Structural features of methyl-accepting taxis proteins conserved between archaeobacteria and eubacteria revealed by antigenic cross-reaction. *J. Bacteriol.* 173:5837–42
- Alam M, Lebert M, Oesterhelt D, Hazelbauer GL. 1989. Methyl-accepting taxis proteins in *Halobacterium halobium*. *EMBO J.* 8:631–39
- Albeck A, Livnah N, Gottlieb H, Sheves M. 1992. ^{13}C NMR studies of model compounds for bacteriorhodopsin: factors affecting the retinal chromophore chemical shifts and absorption maximum. *J. Am. Chem. Soc.* 114:2400–11
- Ames P, Parkinson JS. 1988. Transmembrane signaling by bacterial chemoreceptors: *E. coli* transducers with locked signal output. *Cell* 55:817–26
- Ariki M, Shichida Y, Yoshizawa T. 1987. Low temperature spectrophotometry on the photoreaction cycle of sensory rhodopsin. *FEBS Lett.* 225:255–58
- Asenjo AB, Rim J, Oprian DD. 1994. Molecular determinants of human red/green color discrimination. *Neuron* 12:1131–38
- Barak R, Giebel I, Eisenbach M. 1995. The specificity of fumarate as a switch factor of the bacterial flagellar motor. *Mol. Microbiol.* 19:139–44
- Baselt DR, Fodor SP, Van der Steen R, Lugtenburg J, Bogomolni RA, Mathies RA. 1989. Halorhodopsin and sensory rhodopsin contain a C6-C7 *s-trans* retinal chromophore. *Biophys. J.* 55:193–96
- Baumgartner JW, Kim C, Brissette RE, Inouye M, Park C, Hazelbauer GL. 1994. Transmembrane signaling by a hybrid protein: communication from the domain of chemoreceptor Trg that recognizes sugar-binding proteins to the kinase/phosphatase domain of osmosensor EnvZ. *J. Bacteriol.* 176:1157–63
- Bibikov SI, Grishanin RN, Kaulen AD, Marwan W, Oesterhelt D, Skulachev VP. 1993. Bacteriorhodopsin is involved in halobacterial photoreception. *Proc. Natl. Acad. Sci. USA* 90:9446–50
- Bibikov SI, Grishanin RN, Marwan W, Oesterhelt, Skulachev VP. 1991. The proton pump bacteriorhodopsin is a photoreceptor for signal transduction in *Halobacterium halobium*. *FEBS Lett.* 295:223–26
- Bibikov SI, Skulachev VP. 1989. Mechanisms of phototaxis and aerotaxis in *Halobacterium halobium*. *FEBS Lett.* 243:303–6
- Birge RR. 1990. Nature of the primary photochemical events in rhodopsin and bacteriorhodopsin. *Biochim. Biophys. Acta* 1016:293–327
- Blanck A, Oesterhelt D, Ferrando E, Schegg ES, Lottspeich F. 1989. Primary structure of sensory rhodopsin I, a prokaryotic photoreceptor. *EMBO J.* 8:3963–71
- Bogomolni RA, Spudich JL. 1982. Identification of a third rhodopsin-like pigment in phototactic *Halobacterium halobium*. *Proc. Natl. Acad. Sci. USA* 79:6250–54
- Bogomolni RA, Stoeckenius W, Szundi I, Perozo E, Olson KD, Spudich JL. 1994. Removal of transducer HtrI allows electrogenic proton translocation by sensory rhodopsin I. *Proc. Natl. Acad. Sci. USA* 91:10188–92
- Bousché O, Spudich EN, Spudich JL, Rothschild KJ. 1991. Conformational changes in sensory rhodopsin I: Similarities and differences with bacteriorhodopsin, halorhodopsin, and rhodopsin. *Biochemistry* 30:5395–400
- Chen X, Koshland DE Jr. 1995. The N-terminal cytoplasmic tail of the aspartate receptor is not essential in signal transduction of bacterial chemotaxis. *J. Biol. Chem.* 270:24038–42
- Chervitz SA, Falke JJ. 1995. Lock on/off disulfides identify the transmembrane signaling helix of the aspartate receptor. *J. Biol. Chem.* 270:24043–53
- Chervitz SA, Falke JJ. 1996. Molecular mechanism of transmembrane signaling by the aspartate receptor: a model. *Proc. Natl. Acad. Sci. USA* 93:2545–50
- De Groot HJ, Harbison GS, Herzfeld J, Griffin RG. 1989. Nuclear magnetic resonance study of the Schiff base in bacteriorhodopsin: counterion effects on the ^{15}N shift anisotropy. *Biochemistry* 28:3346–53
- De Groot HJ, Smith SO, Courtin J, Van den Berg E, Winkel C, et al 1990. Solid-state ^{13}C and ^{15}N NMR study of the low pH forms of bacteriorhodopsin. *Biochemistry* 29:6873–83
- Deininger W, Kröger P, Hegemann U, Lottspeich F, Hegemann P. 1995. Chlamyrodopsin represents a new type of sensory photoreceptor. *EMBO J.* 14:5849–58

25. Der A, Szara S, Toth-Boconadi R, Tokaji Z, Keszthelyi L, Stoeckenius W. 1991. Alternative translocation of protons and halide ions by bacteriorhodopsin. *Proc. Natl. Acad. Sci. USA* 88:4751–55
26. Ebrey TG. 1993. Light energy transduction in bacteriorhodopsin. In *Thermodynamics of membranes, receptors and channels*, ed. M Jackson, pp. 353–87. New York: CRC
27. Eisenbach M. 1996. Control of bacterial chemotaxis. *Mol. Microbiol.* 20:903–10
- 27a. Engelhard M, Scharf B, Siebert F. 1996. Protonation changes during the photocycle of sensory rhodopsin II from *Natronobacterium pharaonis*. *FEBS Lett.* 395:195–8
28. Fahmy K, Siebert F, Sakmar TP. 1995. Photoactivated state of rhodopsin and how it can form. *Biophys. Chem.* 56:171–81
29. Ferrando-May E, Brustmann B, Oesterheld D. 1993. A C-terminal truncation results in high-level expression of the functional photoreceptor sensory rhodopsin I in the archaeon *Halobacterium salinarium*. *Mol. Microbiol.* 9:943–53
30. Ferrando-May E, Krah M, Marwan W, Oesterheld D. 1993. The methyl-accepting transducer protein HtrI is functionally associated with the photoreceptor sensory rhodopsin I in the archaeon *Halobacterium salinarium*. *EMBO J.* 12:2999–3005
31. Fodor SP, Gebhard R, Lugtenburg J, Bogomolni RA, Mathies RA. 1989. Structure of the retinal chromophore in sensory rhodopsin I from resonance Raman spectroscopy. *J. Biol. Chem.* 264:18280–83
32. Foster KW, Saranak J, Patel N, Zarilli G, Okabe M, et al 1984. A rhodopsin is the functional photoreceptor for phototaxis in the unicellular eukaryote *Chlamydomonas*. *Nature* 311:756–59
33. Ganter UM, Schmid ED, Perez-Sala D, Rando RR, Siebert F. 1989. Removal of the 9-methyl group of retinal inhibits signal transduction in the visual process. A Fourier transform infrared and biochemical investigation. *Biochemistry* 28:5954–62
34. Gardina PJ, Manson MD. 1996. Attractant signaling by an aspartate chemoreceptor dimer with one cytoplasmic domain. *Science* 274:425–26
35. Gärtner W, Towner P, Hopf H, Oesterheld D. 1983. Removal of methyl groups controls the activity of bacteriorhodopsin. *Biochemistry* 22:2637–44
36. Greenhalgh DA, Farrens DL, Subramaniam S, Khorana HG. 1993. Hydrophobic amino acids in the retinal-binding pocket of bacteriorhodopsin. *J. Biol. Chem.* 268:20305–11
37. Grigorieff N, Ceska TA, Downing KH, Baldwin JM, Henderson R. 1996. Electron-crystallographic refinement of the structure of bacteriorhodopsin. *J. Mol. Biol.* 259:393–421
- 37a. Grishanin RN, Bibikov SI, Altschuler IM, Kaulen AD, Kazimirchuk SB, et al 1996. $\Delta\Psi$ -mediated signalling in the bacteriorhodopsin-dependent photoresponse. *J. Bacteriol.* 178:3008–14
38. Hasselbacher CA, Spudich JL, Dewey TG. 1988. Circular dichroism of halorhodopsin: comparison with bacteriorhodopsin and sensory rhodopsin I. *Biochemistry* 27:2540–46
39. Haupts U, Bamberg E, Oesterheld D. 1996. Different modes of proton translocation by sensory rhodopsin I. *EMBO J.* 15:1834–41
40. Haupts U, Eisefeld W, Stockburger M, Oesterheld D. 1994. Sensory rhodopsin I photocycle intermediate SR1₃₈₀ contains 13-*cis* retinal bound via an unprotonated Schiff base. *FEBS Lett.* 356:25–29
41. Haupts U, Haupts C, Oesterheld D. 1995. The photoreceptor sensory rhodopsin I as a two-photon-driven proton pump. *Proc. Natl. Acad. Sci. USA* 92:3834–38
42. Hazelbauer GL. 1988. The bacterial chemosensory system. *Can. J. Microbiol.* 34:466–74
43. Hazelbauer GL. 1992. Bacterial chemoreceptors. *Curr. Opin. Struct. Biol.* 2:505–10
44. Henderson R, Baldwin JM, Ceska TA, Zemlin F, Beckmann E, Downing KH. 1990. Model for the structure of bacteriorhodopsin based on high-resolution electron cryo-microscopy. *J. Mol. Biol.* 213:899–929
45. Hildebrand E, Schimz A. 1990. The lifetime of photosensory signals in *Halobacterium halobium* and its dependence on protein methylation. *Biochim. Biophys. Acta* 1052:96–105
46. Hildebrand E, Schimz A. 1991. The sensory photoreceptors of *Halobacterium halobium* revisited: action spectra and influence of background light. *Photochem. Photobiol.* 54:1027–37
47. Hirayama J, Imamoto Y, Shichida Y, Kamo N, Tomioka H, Yoshizawa T. 1992. Photocycle of phoborhodopsin from haloalkaliphilic bacterium (*Natronobacterium pharaonis*) studied by low-temperature spectrophotometry. *Biochemistry* 31:2093–98
48. Hirayama J, Imamoto Y, Shichida Y, Yoshizawa T, Asato AE, et al 1994.

- Shape of the chromophore binding site in pharaonis phoborhodopsin from a study using retinal analogs. *Photochem. Photobiol.* 60:388–93
49. Hirayama J, Kamo N, Imamoto Y, Shichida Y, Yoshizawa T. 1995. Reason for the lack of light-dark adaptation in *pharaonis* phoborhodopsin: reconstitution with 13-*cis*-retinal. *FEBS Lett.* 364:168–70
 50. Hoff WD, Dux P, Hård K, Devreese B, Nugteren-Roodzant IM, et al 1994. Thiol ester-linked *p*-coumaric acid as a new photoactive prosthetic group in a protein with rhodopsin-like photochemistry. *Biochemistry* 33:13959–62
 51. Hu J, Griffin RG, Herzfeld J. 1994. Synergy in the spectral tuning of retinal pigments: complete accounting of the opsin shift in bacteriorhodopsin. *Proc. Natl. Acad. Sci. USA* 91:8880–84
 52. Imamoto Y, Shichida Y, Hirayama J, Tomioka H, Kamo N, Yoshizawa T. 1992. Chromophore configuration of *pharaonis* phoborhodopsin and its isomerization on photon absorption. *Biochemistry* 31:2523–28
 53. Imamoto Y, Shichida Y, Hirayama J, Tomioka H, Kamo N, Yoshizawa T. 1992. Nanosecond laser photolysis of phoborhodopsin: from *Natronobacterium pharaonis* appearance of KL and L intermediates in the photocycle at room temperature. *Photochem. Photobiol.* 56:1129–34
 54. Imamoto Y, Shichida Y, Yoshizawa T, Tomioka H, Takahashi T, et al 1991. Photoreaction cycle of phoborhodopsin studied by low-temperature spectrophotometry. *Biochemistry* 30:7416–24
 55. Jung K-H, Spudich JL. 1996. Prototypical residues at the cytoplasmic end of transmembrane helix-2 in the signal transducer HtrI control photochemistry and function of sensory rhodopsin I. *Proc. Natl. Acad. Sci. USA* 93:6557–61
 56. Kataoka M, Mihara K, Kamikubo H, Needleman R, Lanyi JK, Tokunaga F. 1993. Trimeric mutant bacteriorhodopsin, D85N, shows a monophasic CD spectrum. *FEBS Lett.* 333:111–13
 57. Kitajima T, Mukohata U. 1995. Cloning and sequencing of the HtrI gene from *Haloarcula vallismortis*: the HtrI is more similar to HtrI from *Halobacterium salinarium* than HtrII of *Haloarcula vallismortis*. In *Bacterial Rhodopsins Structure, Function and Evolution*, pp. 153–57. Nagoya: Nagoya Univ. Int. Symp.
 58. Krah M, Marwan W, Oesterheld D. 1994. A cytoplasmic domain is required for the functional interaction of SRI and HtrI in archaeal signal transduction. *FEBS Lett.* 353:301–4
 59. Krah M, Marwan W, Vermeglio A, Oesterheld D. 1994. Phototaxis of *Halobacterium salinarium* requires a signalling complex of sensory rhodopsin I and its methyl-accepting transducer HtrI. *EMBO J.* 13:2150–55
 60. Krebs MP, Khorana HG. 1993. Mechanism of light-dependent proton translocation by bacteriorhodopsin. *J. Bacteriol.* 175:1555–60
 61. Krebs MP, Spudich EN, Khorana HG, Spudich JL. 1993. Synthesis of a gene for sensory rhodopsin I and its functional expression in *Halobacterium halobium*. *Proc. Natl. Acad. Sci. USA* 90:3486–90
 62. Krebs MP, Spudich EN, Spudich JL. 1995. Rapid high-yield purification and liposome reconstitution of polyhistidine-tagged sensory rhodopsin I. *Protein Expression and Purification* 6:780–88
 63. Krohs U. 1994. Sensitivity of *Halobacterium salinarium* to attractant light stimuli does not change periodically. *FEBS Lett.* 351:133–36
 64. Krohs U. 1995. Damped oscillations in photosensory transduction of *Halobacterium salinarium* induced by repellent light stimuli. *J. Bacteriol.* 177:3067–70
 65. Lanyi JK. 1990. Halorhodopsin: a light-driven electrogenic chloride transport system. *Physiol. Rev.* 70:319–30
 66. Lanyi JK. 1993. Proton translocation mechanism and energetics in the light-driven pump bacteriorhodopsin. *Biochim. Biophys. Acta* 1183:241–61
 67. Larsen H. 1962. Halophilism. In *The Bacteria*, ed. IC Gunsalus, RY Stanier, pp. 297–342 New York: Academic
 68. Lin SW, Imamoto Y, Fukada Y, Shichida Y, Yoshizawa T, Mathies RA. 1994. What makes red visual pigments red? A resonance Raman microprobe study of retinal chromophore structure in iodopsin. *Biochemistry* 33:2151–60
 69. Lindbeck JC, Goulbourne EA Jr, Johnson MS, Taylor BL. 1995. Aerotaxis in *Halobacterium salinarium* is methylation-dependent. *Microbiology* 141:2945–53
 70. Lucia S, Ascoli C, Petracchi, D. 1992. Photobehavior of *Halobacterium halobium*: sinusoidal stimulation and suppression effect of responses to flashes. *Biophys. J.* 61:1529–39
 71. Lucia S, Ascoli C, Petracchi D, Vanni L. 1989. Motor responses of *Halobacterium halobium* to sinusoidal light stimuli. *Bio-science Reports* 9:481–87

72. Lucia S, Ferraro M, Cercignani G, Petracchi D. 1996. Effects of sequential stimuli on *Halobacterium salinarium* photo-behavior. *Biophys. J.* 71:1554–62
73. Manor D, Hasselbacher CA, Spudich JL. 1988. Membrane potential modulates photocycling rates of bacterial rhodopsins. *Biochemistry* 27:5843–48
74. Marti T, Otto H, Rosselet SJ, Heyn MP, Khorana HG. 1992. Anion binding to the Schiff base of the bacteriorhodopsin mutants Asp-85 → Asn/Asp-212 → Asn and Arg-82 → Gln/Asp-85 → Asn/Asp-212 → Asn. *J. Biol. Chem.* 267:16922–27
75. Marti T, Rosselet SJ, Otto H, Heyn MP, Khorana HG. 1991. The retinylidene Schiff base counterion in bacteriorhodopsin. *J. Biol. Chem.* 266:18674–83
76. Marwan W, Alam M, Oesterheld D. 1991. Rotation and switching of the flagellar motor assembly in *Halobacterium halobium*. *J. Bacteriol.* 173:1971–77
77. Marwan W, Bibikov SI, Montrone M, Oesterheld D. 1995. Mechanism of photosensory adaptation in *Halobacterium salinarium*. *J. Mol. Biol.* 246:493–99
78. Marwan W, Hegemann P, Oesterheld D. 1988. Single photon detection by an Archaeobacterium. *J. Mol. Biol.* 199:663–64
79. Marwan W, Oesterheld D. 1990. Quantitation of photochromism of sensory rhodopsin-I by computerized tracking of *Halobacterium halobium* cells. *J. Mol. Biol.* 215:277–85
80. Marwan W, Oesterheld D. 1991. Light-induced release of the switch factor during photophobic responses of *Halobacterium salinarium*. *Naturwissenschaften* 78:127–29
81. Marwan W, Schäfer W, Oesterheld D. 1990. Signal transduction in *Halobacterium* depends on fumarate. *EMBO J.* 9:355–62
82. Mathies RA, Brito Cruz CH, Pollard WT, Shank CV. 1988. Direct observation of the femtosecond excited-state *cis-trans* isomerization in bacteriorhodopsin. *Science* 240:777–79
83. Mathies RA, Lin SW, Ames JB, Pollard WT. 1991. From femtoseconds to biology: mechanism of bacteriorhodopsin's light-driven proton pump. *Annu. Rev. Biophys. Biophys. Chem.* 20:491–518
84. Mathies RA, Stryer L. 1976. Retinal has a highly dipolar vertically excited state: implications for vision. *Proc. Natl. Acad. Sci. USA* 73:2169–73
85. Matsuno-Yagi A, Mukohata Y. 1977. Two possible roles of bacteriorhodopsin; a comparative study of strains of *Halobacterium halobium* differing in pigmentation. *Biochem. Biophys. Res. Comm.* 78:237–43
86. McBride MJ, Weinberg RA, Zusman DR. 1989. "Frizzy" aggregation genes of the gliding bacterium *Myxococcus xanthus* show sequence similarities to chemotaxis genes of enteric bacteria. *Proc. Natl. Acad. Sci USA* 86:424–28
87. McCain DA, Amici LA, Spudich JL. 1987. Kinetically resolved states of the *Halobacterium halobium* flagellar motor switch and modulation of the switch by sensory rhodopsin I. *J. Bacteriol.* 169:4750–58
88. Merbs SL, Nathans J. 1993. Role of hydroxyl-bearing amino acids in differentially tuning the absorption spectra of the human red and green cone pigments. *Photochem. Photobiol.* 58:706–10
89. Milburn MV, Prive GG, Milligan DL, Scott WG, Yeh J, et al 1991. Three-dimensional structures of the ligand-binding domain of the bacterial aspartate receptor with and without a ligand. *Science* 254:1342–47
90. Miyazaki M, Hirayana J, Hayakawa M, Kamo N. 1992. Flash photolysis study on phoborhodopsin from a halophilic bacterium (*Natronobacterium pharaonis*). *Biochim. Biophys. Acta* 1140:22–29
91. Montrone M, Marwan W, Grunberg H, Musseleck S, Starostzik C, Oesterheld D. 1993. Sensory rhodopsin-controlled release of the switch factor fumarate in *Halobacterium salinarium*. *Mol. Microbiol.* 10:1077–85
92. Mukohata Y. 1994. Comparative studies on ion pumps of the bacterial rhodopsin family. *Biophys. Chem.* 50:191–201
93. Nabor H. 1996. Two alternative models for spontaneous flagellar motor switching in *Halobacterium salinarium*. *J. Theor. Biol.* 181:343–58
94. Nakanishi K, Crouch R. 1995. Application of artificial pigments to structure determination and study of photoinduced transformations of retinal proteins. *Israel J. Chem.* 35:253–72
95. Nordmann B, Lebert MR, Alam M, Nitz S, Kollmannsberger H, et al 1994. Identification of volatile forms of methyl groups released by *Halobacterium salinarium*. *J. Biol. Chem.* 269:16449–54
96. Oesterheld D. 1995. Structure and function of halorhodopsin. *Israel J. Chem.* 35:475–94
97. Oesterheld D, Marwan W. 1993. Signal transduction in halobacteria. In *The Biochemistry of Archaea (Archaeobacteria)*, ed. M Kates, New Comprehensive Bio-

- chemistry Vol. 26, pp. 173–87. Amsterdam: Elsevier Science
98. Oesterhelt D, Stoekenius W. 1973. Functions of a new photoreceptor membrane. *Proc. Natl. Acad. Sci. USA* 70:2853–57
 99. Olson KD, Deval P, Spudich JL. 1992. Absorption and photochemistry of sensory rhodopsin-I: pH effects. *Photochem. Photobiol.* 56:1181–87
 100. Olson KD, Spudich JL. 1993. Removal of the transducer protein from sensory rhodopsin I exposes sites of proton release and uptake during the receptor photocycle. *Biophys. J.* 65:2578–85
 101. Olson KD, Zhang X-N, Spudich JL. 1995. Residue replacements of buried aspartyl and related residues in sensory rhodopsin I: D201N produces inverted phototaxis signals. *Proc. Natl. Acad. Sci. USA* 92:3185–89
 102. Otomo J, Marwan W, Oesterhelt D, Desel H, Uhl R. 1989. Biosynthesis of the two halobacterial light sensors P₄₈₀ and sensory rhodopsin and variation in gain of their signal transduction chains. *J. Bacteriol.* 171:2155–59
 103. Otomo J, Tomioka H, Urabe Y, Sasabe H. 1992. Properties and the primary structures of new bacterial rhodopsins. In *Structures and Functions of Retinal Proteins*, ed. JL Rigaud, Colloque INSERM, Vol. 221, pp. 105–8. London: John Libbey Eurotext
 104. Otomo J, Urabe Y, Tomioka H, Sasabe H. 1992. The primary structures of helices A to G of three new bacteriorhodopsin-like retinal proteins. *J. Gen. Microbiol.* 138:2389–96
 105. Parkinson JS. 1993. Signal transduction schemes of bacteria. *Cell* 73:857–71
 106. Perazzona B, Spudich EN, Spudich JL. 1996. Deletion mapping of the sites on the HtrI transducer for sensory rhodopsin I interaction. *J. Bacteriol.* 178:6475–78
 107. Petracchi D, Lucia S, Cercignani G. 1994. Photobehaviour of *Halobacterium halobium*: proposed models for signal transduction and motor switching. *J. Photochem. Photobiol. B: Biol.* 24:75–99
 108. Pulvermüller A, Palczewski K, Hofmann KP. 1993. Interaction between photoactivated rhodopsin and its kinase: stability and kinetics of complex formation. *Biochemistry*, 32:14082–88
 109. Rao R, Oprian DD. 1996. Activating mutations of rhodopsin and other G protein-coupled receptors. *Annu. Rev. Biophys. Biomol. Struct.* 25:287–314
 110. Rath P, Olson KD, Spudich JL, Rothschild KJ. 1994. The Schiff base counterion of bacteriorhodopsin is protonated in sensory rhodopsin I: spectroscopic and functional characterization of the mutated proteins D76N and D76A. *Biochemistry* 33:5600–6
 111. Rath P, Spudich EN, Neal DD, Spudich JL, Rothschild KJ. 1996. Asp76 is the Schiff base counterion and proton acceptor in the proton translocating form of sensory rhodopsin I. *Biochemistry* 35:6690–96
 112. Rothschild KJ. 1992. FTIR difference spectroscopy of bacteriorhodopsin: toward a molecular model. *J. Bioenerg. Biomembr.* 24:147–67
 113. Rudolph J, Oesterhelt D. 1995. Chemotaxis and phototaxis require a CheA histidine kinase in the archaeon *Halobacterium salinarium*. *EMBO J.* 14:667–73
 114. Rudolph J, Oesterhelt D. 1996. Deletion analysis of the *che* operon in the Archaeon *Halobacterium salinarium*. *J. Mol. Biol.* 258:548–54
 115. Rudolph J, Tolliday N, Schmitt C, Schuster SC, Oesterhelt D. 1995. Phosphorylation in halobacterial signal transduction. *EMBO J.* 14:4249–57
 116. Sasaki J, Brown LS, Chon YS, Kandori H, Maeda A, et al 1995. Conversion of bacteriorhodopsin into a chloride ion pump. *Science* 269:73–75
 117. Scharf B, Engelhard M, Siebert F. 1992. A carboxyl group is protonated during the photocycle of the photophobic receptor psR-II from *Natronobacterium pharaonis*. See Ref. 103, pp. 317–20
 118. Scharf B, Hess B, Engelhard M. 1992. Chromophore of sensory rhodopsin II from *Halobacterium halobium*. *Biochemistry* 31:12486–92
 119. Scharf B, Pevec B, Hess B, Engelhard M. 1992. Biochemical and photochemical properties of the photophobic receptors from *Halobacterium halobium* and *Natronobacterium pharaonis*. *Eur. J. Biochem.* 206:359–66
 120. Scharf B, Wolff EK. 1994. Phototactic behaviour of the archaeobacterial *Natronobacterium pharaonis*. *FEBS Lett.* 340:114–16
 121. Schegk ES, Oesterhelt D. 1988. Isolation of a prokaryotic photoreceptor: sensory rhodopsin from halobacteria. *EMBO J.* 7:2925–33
 122. Schimz A, Hildebrand E. 1989. Periodicity and chaos in the response of *Halobacterium salinarium* to temporal light gradients. *Eur. Biophys. J.* 17:237–43
 123. Schimz A, Hildebrand E. 1992. Nonrandom structures in the locomotor behavior of *Halobacterium*: a bifurcation route

- to chaos? *Proc. Natl. Acad. Sci. USA* 89:457-60
124. Schobert B, Lanyi JK. 1982. Halorhodopsin is a light-driven chloride pump. *J. Biol. Chem.* 257:10306-13
 125. Schoenlein RW, Peteanu LA, Mathies RA, Shank CV. 1991. The first step in vision: femtosecond isomerization of rhodopsin. *Science* 254:412-15
 126. Seidel R, Scharf B, Gautel M, Kleine K, Oesterhelt D, Engelhard M. 1995. The primary structure of sensory rhodopsin II: a member of an additional retinal protein subgroup is coexpressed with its transducer, the halobacterial transducer of rhodopsin II. *Proc. Natl. Acad. Sci. USA* 92:3036-40
 127. Seligman L, Manoil C. 1994. An amphipathic sequence determinant of membrane protein topology. *J. Biol. Chem.* 269:19888-96
 128. Seligman L, Bailey J, Manoil C. 1995. Sequences determining the cytoplasmic localization of a chemoreceptor domain. *J. Bacteriol.* 177:2315-20
 129. Senger H, Schmidt W. 1994. Diversity of photoreceptors. In *Photomorphogenesis in Plants*, ed. RE Kendrick, GHM Kronenberg, pp. 301-25. Dordrecht: Kluwer Academic
 130. Shichida Y, Imamoto Y, Yoshizawa T, Takahashi T, Tomioka H, Kamo N, Kobatake Y. 1988. Low-temperature spectrophotometry of phoborhodopsin. *FEBS Lett.* 236:333-36
 131. Small GD, Min B, Lefebvre PA. 1995. Characterization of a *Chlamydomonas reinhardtii* gene encoding a protein of the DNA photolyase/blue light photoreceptor family. *Plant Mol. Biol.* 28:443-54
 132. Soppa J, Duschl J, Oesterhelt D. 1993. Bacterioopsin, haloopsin, and sensory opsin I of the halobacterial isolate *Halobacterium* sp. strain SG1: three new members of a growing family. *J. Bacteriol.* 175:2720-26
 133. Sprenger WW, Hoff WD, Armitage JP, Hellingwerf KJ. 1993. The eubacterium *Ectothiorhodospira halophila* is negatively phototactic, with a wavelength dependence that fits the absorption spectrum of the photoactive yellow protein. *J. Bacteriol.* 175:3096-104
 134. Spudich EN, Hasselbacher CA, Spudich JL. 1988. A methyl-accepting protein associated with bacterial sensory rhodopsin I. *J. Bacteriol.* 170:4280-85
 135. Spudich EN, Spudich JL. 1993. The photochemical reactions of sensory rhodopsin I are altered by its transducer. *J. Biol. Chem.* 268:16095-97
 136. Spudich EN, Takahashi T, Spudich JL. 1989. Sensory rhodopsins I and II modulate a methylation/demethylation system in *Halobacterium halobium* phototaxis. *Proc. Natl. Acad. Sci. USA* 20:7746-50
 137. Spudich JL. 1993. Color sensing in the *Archaea*: a eukaryotic-like receptor coupled to a prokaryotic transducer. *J. Bacteriol.* 157:7755-61
 138. Spudich JL. 1994. Protein-protein interaction converts a proton pump into a sensory receptor. *Cell* 79:747-50
 139. Spudich JL. 1995. The transducer protein HtrI controls proton movements in sensory rhodopsin I. *Biophys. Chem.* 56:165-69
 140. Spudich JL, Bogomolni RA. 1984. The mechanism of colour discrimination by a bacterial sensory rhodopsin. *Nature* 312:509-13
 141. Spudich JL, Bogomolni RA. 1988. Sensory rhodopsins of halobacteria. *Annu. Rev. Biophys. Biophys. Chem.* 17:193-215
 142. Spudich JL, Lanyi JK. 1996. Shuttling between protein conformations: the common mechanism for sensory transduction and ion transport. *Curr. Opin. Cell Biol.* 8:452-57
 143. Spudich JL, Zacks DN, Bogomolni RA. 1995. Microbial sensory rhodopsins: photochemistry and function. *Israel J. Chem.* 35:495-513
 144. Stock JB, Surette MG. 1996. Chemotaxis. In *Escherichia coli and Salmonella typhimurium*, ed. FC Neidhardt, pp 1103-29. Washington DC: ASM Press
 145. Stoeckenius W, Wolff EK, Hess B. 1988. A rapid population method for action spectra applied to *Halobacterium halobium*. *J. Bacteriol.* 170:2790-95
 146. Subramaniam S, Gerstein M, Oesterhelt D, Henderson R. 1993. Electron diffraction analysis of structural changes in the photocycle of bacteriorhodopsin. *EMBO J.* 12:1-8
 147. Subramaniam S, Marti T, Khorana HG. 1990. Protonation state of Asp (Glu)-85 regulates the purple-to-blue transition in bacteriorhodopsin mutants Arg-82 → Ala and Asp-85 → Glu: the blue form is inactive in proton translocation. *Proc. Natl. Acad. Sci. USA* 87:1013-17
 148. Sundberg SA, Alam M, Lebert M, Spudich JL, Oesterhelt D, Hazelbauer GL. 1990. Characterization of mutants of *Halobacterium halobium* defective in taxis. *J. Bacteriol.* 172:2328-35
 149. Swanson RV, Alex LA, Simon MI. 1994. Histidine and aspartate phosphorylation: two-component systems and the limits of

- homology. *Trends Biochem. Sci.* 19:485–90
150. Szundi I, Bogomolni RA. 1996. Early photochemistry shows the involvement of aspartate 76 residue in sensory rhodopsin I function. *Biophys. J.* 70:A358
 151. Takahashi T. 1992. Automated measurement of movement responses in *Halobacterium*. In *Image Analysis in Biology*, ed. D-P Häder, pp. 315–28. Boca Raton: CRC
 152. Takahashi T, Tomioka H, Kamo N, Kobatake Y. 1985. A photosystem other than PS370 also mediates the negative phototaxis of *Halobacterium halobium*. *FEMS Microbiol. Lett.* 28:161–64
 153. Takahashi T, Yan B, Mazur P, Derguini F, Nakanishi K, Spudich JL. 1990. Color regulation in the archaeobacterial phototaxis receptor phoborhodopsin (sensory rhodopsin II). *Biochemistry* 29:8467–74
 154. Takahashi T, Yan B, Spudich JL. 1992. Sensitivity increase in the photophobic response of *Halobacterium halobium* reconstituted with retinal analogs: a novel interpretation for the fluence-response relationship and a kinetic model. *Photochem. Photobiol.* 56:1119–28
 155. Tatsuno I, Homma M, Oosawa K, Kawagishi I. 1996. Signaling by the *Escherichia coli* aspartate chemoreceptor Tar with a single cytoplasmic domain per dimer. *Science* 274:423–24
 156. Tomioka H, Sasabe H. 1995. Isolation of photochemically active archaeobacterial photoreceptor, *pharaonis* phoborhodopsin from *Natronobacterium pharaonis*. *Biochim. Biophys. Acta* 1234:261–67
 157. Tomioka H, Takahashi T, Kamo N, Kobatake Y. 1986. Action spectrum of the photoattractant response of *Halobacterium halobium* in early logarithmic growth phase and the role of sensory rhodopsin. *Biochim. Biophys. Acta* 884:578–84
 158. Tomioka H, Takahashi T, Kamo N, Kobatake Y. 1986. Flash spectrophotometric identification of a fourth rhodopsin-like pigment in *Halobacterium halobium*. *Biochem. Biophys. Res. Comm.* 139:389–95
 159. Wagner G, Hesse V, Traulich B. 1991. Steady hypsochromic shift of peak responsivity to attractant light from 590 nm to 560 nm in *Halobacterium halobium*. *Photochem. Photobiol.* 53:701–6
 160. Wagner G, Rothärmel T, Traulich B. 1991. Retinal-opsin-dependent detection of short-wavelength ultraviolet radiation (UV-B), and endogenous bias on direction of flagellar rotation in tethered *Halobacterium halobium* cells. In *General and Applied Aspects of Halophilic Microorganisms*, ed. F Rodriguez-Valera, pp. 139–47. New York: Plenum
 161. Wang Q, Schoenlein RW, Peteanu LA, Mathies RA, Shank CV. 1994. Vibrationally coherent photochemistry in the femtosecond primary event of vision. *Science* 266:422–24
 162. Yan B, Cline SW, Doolittle F, Spudich JL. 1992. Transformation of a Bop-Hop-Sop-I-Sop-II- *Halobacterium halobium* mutant to Bop⁺: effects of bacteriorhodopsin photoactivation on cellular proton fluxes and swimming behavior. *Photochem. Photobiol.* 56:553–61
 163. Yan B, Nakanishi K, Spudich JL. 1991. Mechanism of activation of sensory rhodopsin I: evidence for a steric trigger. *Proc. Natl. Acad. Sci. USA* 88:9412–16
 164. Yan B, Spudich EN, Sheves M, Steinberg G, Spudich JL. 1997. Complexation of the signal transducing protein HtrI to sensory rhodopsin I and its effect on thermodynamics of signaling state deactivation. *J. Phys. Chem.* 101:109–13
 165. Yan B, Spudich JL. 1991. Evidence that the repellent receptor form of sensory rhodopsin I is an attractant signaling state. *Photochem. Photobiol.* 54:1023–26
 166. Yan B, Spudich JL, Mazur P, Vunnam S, Derguini F, Nakanishi K. 1995. Spectral tuning in bacteriorhodopsin in the absence of counterion and coplanarization effects. *J. Biol. Chem.* 270:29668–70
 167. Yan B, Takahashi T, Johnson R, Derguini F, Nakanishi K, Spudich JL. 1990. All-trans/13-cis isomerization of retinal is required for phototaxis signaling by sensory rhodopsins in *Halobacterium halobium*. *Biophys. J.* 57:807–14
 168. Yan B, Takahashi T, Johnson R, Spudich JL. 1991. Identification of signaling states of a sensory receptor by modulation of lifetimes of stimulus-induced conformations: the case of sensory rhodopsin II. *Biochemistry* 30:10686–92
 169. Yan B, Takahashi T, McCain DA, Rao VJ, Nakanishi K, Spudich JL. 1990. Effects of modifications of the retinal β -ionone ring on archaeobacterial sensory rhodopsin I. *Biophys. J.* 57:477–83
 170. Yan B, Xie A, Nienhaus GU, Katsuta Y, Spudich JL. 1993. Steric constraints in the retinal binding pocket of sensory rhodopsin I. *Biochemistry* 32:10224–32
 171. Yao VJ, Spudich EN, Spudich JL. 1994. Identification of distinct domains for sig-

- naling and receptor interaction of the sensory rhodopsin I transducer, HtrI. *J. Bacteriol.* 176:6931–35
172. Yao VJ, Spudich JL. 1992. Primary structure of an archaeobacterial transducer, a methyl-accepting protein associated with sensory rhodopsin I. *Proc. Natl. Acad. Sci. USA* 89:11915–19
173. Zhang W, Brooun A, McCandless J, Banda P, Alam M. 1996. Signal transduction in the Archaeon *Halobacterium salinarium* is processed through three subfamilies of 13 soluble and membrane-bound transducer proteins. *Proc. Natl. Acad. Sci. USA* 93:4649–54
174. Zhang W, Brooun A, Müller MM, Alam M. 1996. The primary structures of the Archaeon *Halobacterium salinarium* blue light receptor sensory rhodopsin II and its transducer, a methyl-accepting protein. *Proc. Natl. Acad. Sci. USA* 93:8230–35